Foreword to

Professional Team Demonstration Uncertainty/Sensitivity Analysis

In general terms, the demonstration study of Sensitivity and Uncertainty Analysis concerns producing INPUT for computer models and then analyzing the corresponding OUTPUT to determine the extent of influence the input variables have on the magnitude and uncertainty of the output responses. The Demonstration Analysis has the following specific objectives:

1. Provide an explicit example of the use of state of the art statistical methods for performing sensitivity and uncertainty analysis in a context of direct interest to the Commission.

2. Illustrate the implementation of Latin hypercube sampling for adaptation by the modelers to their proprietary, operational models.

3. Provide the rationale for Form F to be added to Module 3 that will complement the existing Form B regarding wind speeds.

The techniques described in the Demonstration Analysis apply to *any* computer model so the focus is on the sampling method used to determine the INPUT and the analysis techniques used to determine the impacts on the OUTPUT. The computer model gives a framework for illustration but is not of interest in itself and hence, should not be the centerpiece of discussion. For example the Rankine-vortex wind field, linear decay and cubic damage relationships are surrogates or place-holders for actual operational modules that the Professional Team is precluded from using in a public domain. Each of these surrogates could be replaced by a realistic module without change to the manner in which the input is generated or the manner in which the input-output relationships are assessed. Of course, replacing one or more model surrogates would change the specific numerical values generated but here again, it is the output graphical and numerical products that are of interest. The sensitivity and uncertainty analysis methodology demonstrated in the report provide a sound approach to assessing computer models.

Acknowledgements

The demonstration study was originally conceived at the professional team meeting June 6-7, 2001 hosted by John Pepper in Weston, Florida. At this meeting, a brainstorming session on the merits and particulars of a study took place, culminating in an initial specification of ranges and distributions for the input variables. Professional team members in this session were:

Mark Brannon, actuary
Paul Fishwick, computer scientist
Ronald Iman, statistician
Mark Johnson, statistician
Richard Nance, computer scientist
John Pepper, engineer
Peter Ray, meteorologist
Tom Schroeder, meteorologist
Martin Simons, actuary
Fred Stolaski, engineer

State Board of Administration staff were present and helped greatly in maintaining the momentum of the meeting. Following the meeting, a proposal to carry out the demonstration was prepared and then presented to the Commission on July 30-31, 2001.

The proposal was approved by the commission, culminating in this report. The authors are grateful for many useful comments from professional team members. John Pepper provided particularly valuable insights on vulnerability aspects, and Martin Simons offered numerous improvements while helping us to keep our focus on the objectives of the study.

Professional Team Demonstration Uncertainty/Sensitivity Analysis

Ronald L. Iman, Ph.D.
Southwest Technology Consultants
Albuquerque, NM

Mark E. Johnson, Ph.D.
University of Central Florida
Orlando, FL

Tom A. Schroeder, Ph.D.
University of Hawaii
Honolulu, HI

Introduction. During its June 5-6 2001 meeting in Ft. Lauderdale, the Professional Team developed sample meteorology characteristics to serve as the basis for a demonstration uncertainty and sensitivity analysis (UA/SA). The Professional Team felt that a demonstration could serve as a template to guide modelers in complying with the Commission's Year 2000 Standards 5.6.3 and 5.6.4. Details of the proposed analysis were presented to the Commission at its July 30, 2001 meeting and approval was received for a developing a demonstration analysis. The working definitions of sensitivity and uncertainty analysis used in the document are as follows.

Sensitivity analysis: Determination of the change in response of a model to changes in model inputs and specifications

Uncertainty analysis: Determination of the variation or imprecision in model output resulting from the collective variation in the model inputs

The completed demonstration results appear in this report and a summary will be presented to the Commission at their scheduled September 18-19, 2001 meeting. Following the presentation of the results, it is anticipated that the Commission, with advisement by the Professional Team, can determine sample input characteristics that modelers would utilize as part of the application process.

Specifically, the Professional Team would develop files containing sample input characteristics approved by the Commission. These files would be given to the modelers, who would run them and provide corresponding output files with their submissions in the same sense as is currently being done for Form B. The Professional Team could then use these input-output files to perform its own sensitivity and uncertainty analyses prior to onsite audits. Finally, with each modeler using the same input, the output files could be useful in making model-to-model comparisons if so desired by the Commission.

Figure 1 shows a schematic representation of the demonstration input-output process. A sample of size n=100 is selected for each of four input characteristics. This sample is used as input to the wind speed computer model, which is the Rankine-vortex model in this demonstration analysis. Wind velocity is computed hourly for 12 hours for each of the 100 sets of four input characteristics. The calculated wind speeds are used as input to surrogate damage function model and the damage is converted to loss cost. The goal of the sensitivity analysis is to determine which of the input X's influence wind velocity at time t and max lost cost. The goal of the uncertainty analysis is to determine which of the input X's contribute to the uncertainty in the wind velocity at time t and max lost cost.

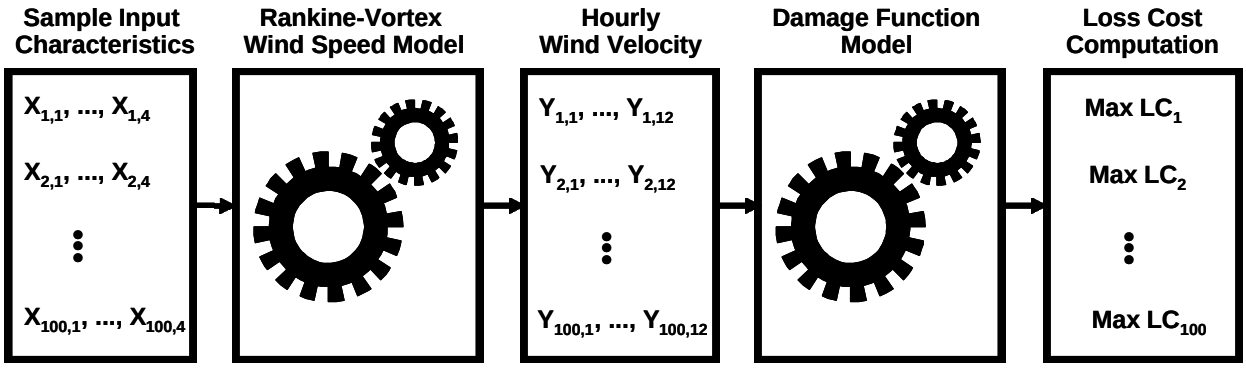

Figure 1. Schematic Representation of the Input-Output Process for the UA/SA Process

The remaining sections of this report will:

- Define the tracking and exposure grid used in the demonstration UA/SA
- Define sample input characteristics and probability distributions used to characterize their uncertainties
- Assess the plausible correlations among input probability distributions
- Present the Rankine-vortex function that was used to calculate wind velocities through the grid and summarize the calculated wind velocities
- Define standardized regression coefficients (SRC) and partial correlation coefficients (PCC) that are used in the demonstration analysis as measures of relative influence of the sample input characteristics
- Illustrate the calculation and interpretation of SRCs and PCCs with an example
- Display sensitivity measures versus time
- Present the details of a simplified loss cost function used to convert wind velocities in the analysis to loss cost
- Illustrate sensitivity analysis applied to loss costs
- Define uncertainty importance (UI) as a measure of the relative contribution to the uncertainty in the sample input characteristics
- Illustrate the calculation and interpretation of UIs with an example
- Illustrate uncertainty analysis applied to loss cost
- Summarize the results of the demonstration UA/SA and their implication on the Commission standards and modules

Objective of the Demonstration Analysis. It must be emphasized that the results presented in this report are intended to demonstrate the application of statistical sampling methods in the areas of meteorology and loss cost estimation. The concrete example utilized in this demonstration should greatly facilitate the implementation of Latin Hypercube Sampling methods. The "black-box" demonstration model is utilized to illustrate setting up the input variables (determining which computer runs are to be made) and to illustrate the graphical and numerical summary products possible for assessing the input-output variable relationships (both sensitivity and uncertainty). The black-box used here is by no means a black-box, but a simple Rankine-vortex windfield with linear decay, a cubic damage function, and a simple 1% deductible with 50% damage equating to 100% insured loss. Aspects of this simple model do not compete with sophisticated modules in commercial modules. However, the process of performing the sensitivity and uncertainty analysis carries over to the proprietary models. Of particular concern could be the cubic damage function, which has zero damage at 50mph, complete damage at 140mph and a cubic function in between (Equation 12). This damage function is provided to move the UA/SA from wind speeds to loss costs. The intent is not to focus on the damage or insurance "module" per se, but rather to consider the demonstration study as it relates to general sensitivity and uncertainty analyses.

Tracking Grid. The demonstration analysis included results for Category 1 and Category 5 hurricanes using the Rankine-vortex function (details presented later) to make wind velocity determinations. These determinations were made at each vertex in a 5×13 grid (65 vertices) that follows the path of the hurricane along an area 20mi wide and 180mi long. This grid is illustrated in Figure 2.

Hurricane tracking started at (0, 0) in the grid in Figure 2. These coordinates are located directly offshore 15 miles east of Miami. Miami has coordinates (15, 0). At time t = 0hr, the eye of the hurricane has coordinates (0, 0) with a westerly heading. Wind field speed calculations were made hourly for 12hr at each vertex in the grid.

The Professional Team selected sample meteorology characteristics to be used, their ranges, and distributions. Those characteristics are now described.

Input Sample Characteristics. The Professional Team selected central pressure (CP), radius of maximum winds (Rmax), forward speed (V_T), and far field pressure (FFP) as input characteristics of interest as illustrated in the first box of Figure 1. Each of these characteristics (parameters) has an associated degree of uncertainty for a specific storm. Table 1 summarizes the ranges of uncertainty ascribed to the sample meteorology input characteristics by the Professional Team for each hurricane category.

Since forward speed varies from 10 to 20 mph during the 12hr period for both Category 1 and Category 5, the eye of the storm will move from (0, 0) to (120, 0) with V_T = 10 mph and from (0, 0) to (240, 0) with V_T = 20 mph. The mean forward speed (15mph) moves the eye from (0, 0) to (180, 0).

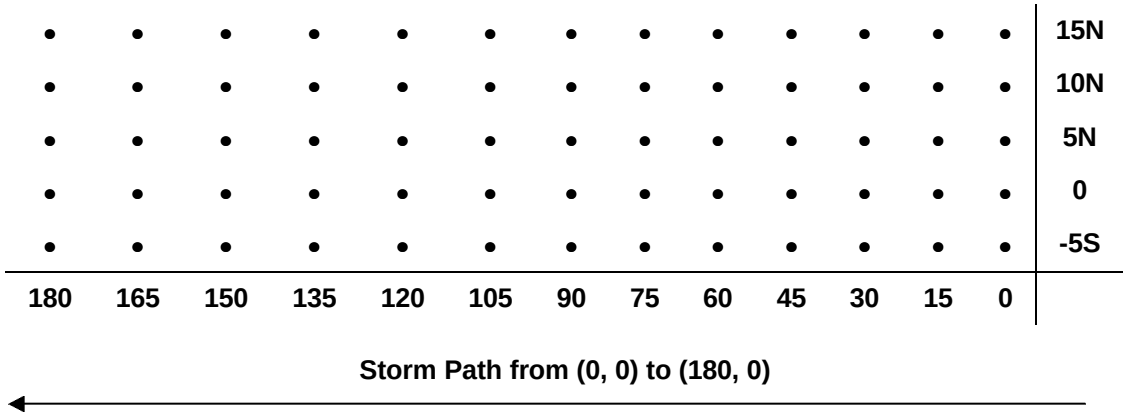

Figure 2. Tracking Grid Along (X,0) for Calculating Hourly Wind Velocities

Table 1. Ranges of Uncertainty for Meteorology Input Sample Characteristics Used in the Demonstration UA/SA

	Category 1	Category 5
Central pressure	980mB ≤ CP ≤ 990mB	900mB ≤ CP ≤ 920mB
Radius of max wind	12mi ≤ Rmax ≤ 21mi	6mi ≤ Rmax ≤ 12mi
Forward speed	10mph ≤ V_T ≤ 20mph	10mph ≤ V_T ≤ 20mph
Far field pressure	1010mB ≤ FFP ≤ 1016mB	1010mB ≤ FFP ≤ 1016mB

The uncertainties in the sample input characteristics in Table 1 were characterized with triangular probability distributions. The parameters of these distributions are given in Table 2. The means and standard deviations in Table 2 are determined by Equations 1 and 2.

$$Mean = \frac{a+b+c}{3} \tag{1}$$

$$St\ Dev = \sqrt{\frac{a(a-b)+b(b-c)+c(c-a)}{18}} \tag{2}$$

Table 2. Parameters of Triangular Distributions Used to Characterize the Uncertainty in the Input Sample Characteristics in Table 1

	Category 1			Category 5		
	Parameters	**Mean**	**St Dev**	**Parameters**	**Mean**	**St Dev**
CP	a=980 b=985 c=990	985	2.04	a=900 b=910 c=920	910	4.08
Rmax	a=12 b=15 c=21	16	1.87	a=6 b=8 c=12	8.67	1.25
V_T	a=10 b=15 c=20	15	2.04	a=10 b=15 c=20	15	2.04
FFP	a=1010 b=1013 c=1016	1013	1.22	a=1010 b=1013 c=1016	1013	1.22

Simple Correlation. The Professional Team discussed the possibility of CP and Rmax having some degree of correlation or linear relationship, particularly for a Category 5 hurricane. A commonly used measure of the degree of linear relationship between two variables is the simple correlation coefficient, which varies between -1 and +1 with a negative correlation indicative of one variable increasing while the other is decreasing. On the other hand, a positive correlation indicates that the two variables jointly increase or decrease. Equation 3 gives the formula for computing the simple correlation coefficient for bivariate variables X and Y based on a random sample of size n.

$$r = \frac{\sum_{i=1}^{n}(X_i - \overline{X})(Y_i - \overline{Y})}{\sqrt{\sum_{i=1}^{n}(X_i - \overline{X})^2 \sum_{i=1}^{n}(Y_i - \overline{Y})^2}} \tag{3}$$

As a result of the Professional Team's discussion, the sample correlation between CP and Rmax was set at 0.50 for a Category 5 and as 0.25 for a Category 1. All other pairs of input parameters were uncorrelated. A Latin hypercube sample (LHS) (see Iman 1999 summary article in Appendix A for details) of size n=100 was generated using the sample characteristics given in Table 2. The target correlations between CP and Rmax were 0.25 for a Category 1 and 0.50 for a Category 5 (Iman and Conover, 1982 and Iman and Davenport, 1982). The target correlation was 0.00 for all other pairs of input parameters.

The actual pairwise correlations for the LHS based on Equation 3 are given in Table 3. Note that the sample correlations for CP and Rmax are 0.25 for Category 1 and 0.49 for Category 5, which are very close to their target values. Note that the other (off-diagonal) pairwise correlations are all close to their desired value, 0.00.

Table 3. Simple Correlations for Category 5 Sample Values

Category 1

CP	1.000	0.250	0.006	-0.007
Rmax	0.250	1.000	-0.013	0.025
V_T	0.006	-0.013	1.000	0.007
FFP	-0.007	0.025	0.007	1.000
	CP	**Rmax**	**V_T**	**FFP**

Category 5

CP	1.000	0.490	0.005	-0.012
Rmax	0.490	1.000	-0.012	-0.009
V_T	0.005	-0.012	1.000	0.006
FFP	-0.012	-0.009	0.006	1.000
	CP	**Rmax**	**V_T**	**FFP**

Figures 3 and 4 show scatterplots of the sampled values of CP and Rmax for Category 1 and 5, respectively. Note that these graphs show a slight tendency for CP and Rmax to increase together, more so in Figure 4 than in Figure 3. That is, there is slight linear relationship indicated between these two sample characteristics, as expected from their prescribed correlation.

Rankine Vortex Function. The wind velocity was calculated hourly at each vertex in the 5 $\times$ 13 grid shown in Figure 1 for each of the n=100 LHS values. These calculations were based on the Rankine-vortex function (Holliday 1969) which uses the values of CP, Rmax, V_T, and FFP in the LHS. The calculation of the wind velocity (V_{Total}) at an arbitrary point (x, y) in the storm-centered coordinate system is now explained.

For a Rankine vortex, the tangential wind velocity function (see Figure 5) is

$$\begin{aligned} V_q(r) &= \frac{V_{\max}}{R_{\max}} r & 0 \le r \le R_{\max} \\ &= V_{\max}\left(\frac{R_{\max}}{r}\right)^{0.6} & r \ge R_{\max} \end{aligned} \tag{4}$$

where

$$V_{\max} = 14 * 1.15\sqrt{FFP - CP} \quad - V_T \tag{5}$$

The rankine vortex wind model (See Figure 6) is a combination of a linear increase in wind as a function of the radius in the inner core (often termed solid-body rotation) and a hyperbolic decrease in wind speed beyond the

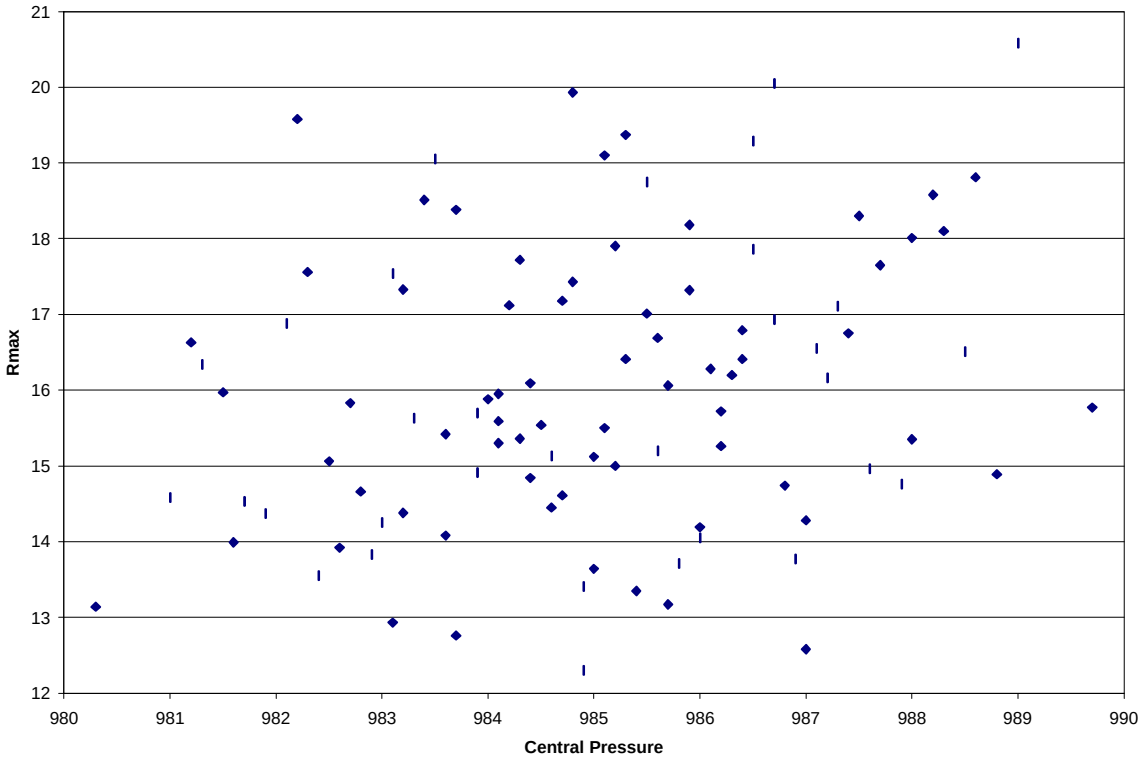

Figure 3. A Scatterplot of Rmax versus Central Pressure with a Correlation of 0.25

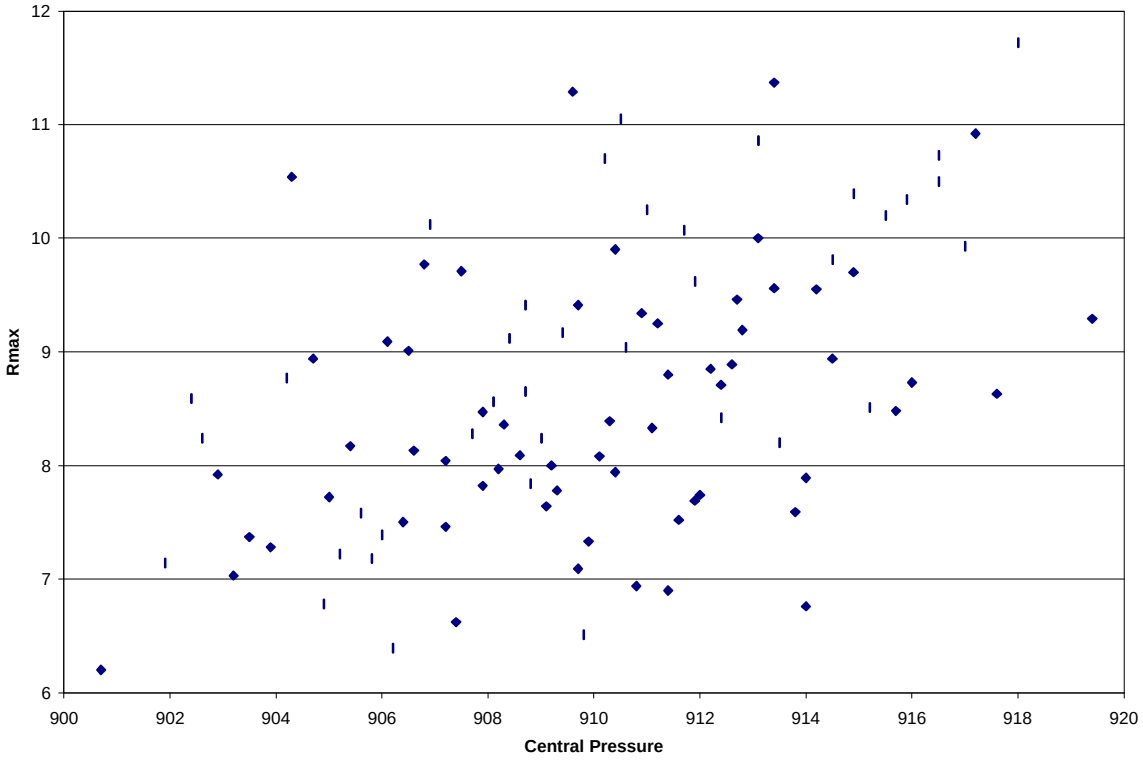

Figure 4. A Scatterplot of Rmax versus Central Pressure with a Correlation of 0.5

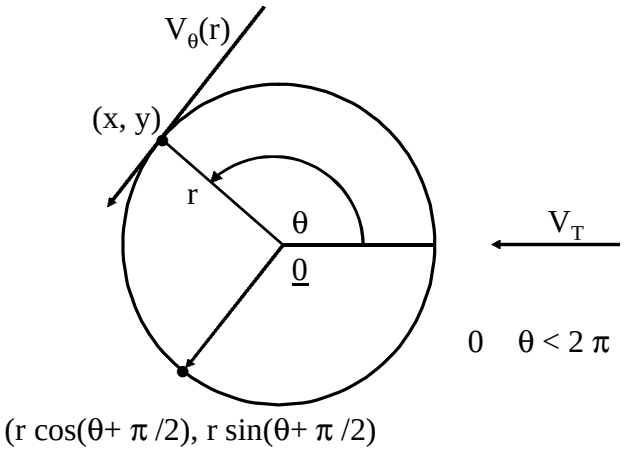

Figure 5. Tangential Wind Velocity Vector

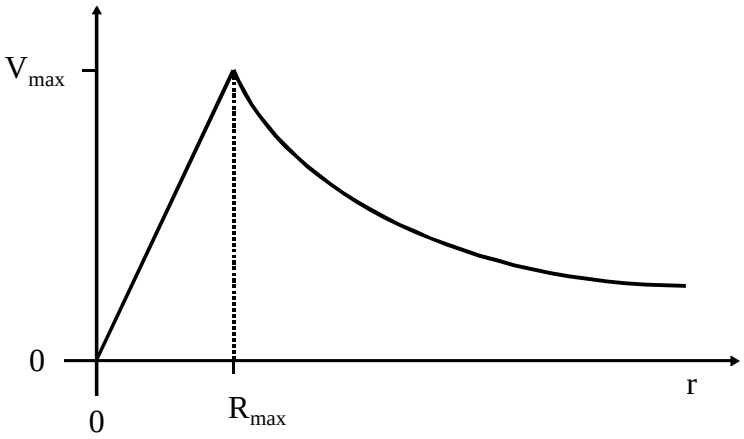

Figure 6. Rankine Vortex Function

radius of maximum winds (the classical Rankine vortex). In ideal cases (inviscid flow) the profile is VR = constant whereas in real cases the profile is VR (to some power A) = constant. Empirical values of A range from 0.5 to 0.6 (Anthes, 1982, Fletcher, Redmond, Barnes, and Schroeder, 1995). Physically the result is equivalent to the flow in a cylindrical tank of water within which a hollow cylinder rotates.

Note that FFP in Equation 5 is commonly set equal to 1013mB, but the uncertainty in FFP is incorporated into this demonstration analysis. Also, the factor 1.15 is used to convert knots to mph. The wind velocity function (see Figure 6) is given by

$$V_{Total}(x,y) = \sqrt{\left[V_q(r)\cos\left(q+\frac{p}{2}\right) - V_T\right]^2 + \left[V_q(r)\sin\left(q+\frac{p}{2}\right)\right]^2} \quad (6)$$

where

$$r = \sqrt{x^2 + y^2} \quad (7)$$

$$q = \tan^{-1}\left(\frac{y}{x}\right) \quad adjusted\ so\ 0 \le q < 2p \quad (8)$$

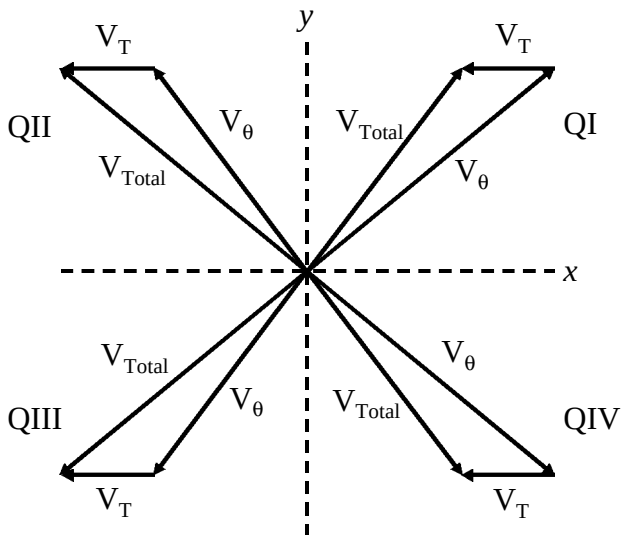

Figure 7. (*x*, *y*) Locations for $V_{Total} = V_\theta + V_T$

Note: $x = r \cos\theta$, $y = r \sin\theta$, and $(\cos(\theta + \pi/2), \sin(\theta + \pi/2))$ is the tangential wind direction.

Footnote on $\tan^{-1}(\theta)$ "adjustment" to get θ into the correct $(0, 2\pi)$ range for evaluating V_{Total}:

$$\theta = \begin{cases} \tan^{-1}(y/x) & x > 0,\ y > 0 \quad \text{Quadrant I} \\ \pi + \tan^{-1}(y/x) & x < 0 \quad \text{Quadrants II and III} \\ 2\pi + \tan^{-1}(y/x) & x > 0,\ y < 0 \quad \text{Quadrant IV} \\ \pi/2 & x = 0,\ y > 0 \\ 3\pi/2 & x = 0,\ y < 0 \\ \text{undefined} & x = 0,\ y = 0 \end{cases}$$

V_θ, the tangential wind vector is a $\pi/2$ rotation of the (*x, y*) location (see Figure 6). For "west" moving storms, the forward movement represented by the V_T vector yields:

V_{Total} length > V_θ length for (*x, y*) right of the line of movement
V_{Total} length < V_θ length for (*x, y*) left of the line of movement

Obviously, careful attention to signs of the coordinates of $(\cos(3 + \pi/2), \sin(3 + \pi/2))$ is essential.

Summary of Calculated Wind Velocities. V_{Total} was calculated hourly at each vertex in the grid shown in Figure 2 for each of the n=100 LHS values. Thus, a total of $5 \times 13 \times 13\text{hr} \times 100$ samples = 84,500 calculations were made for V_{Total} for both the Category 1 and Category 5 hurricanes. These calculated values are displayed in histograms in Figures 8 and 9 for Category 1 and 5, respectively. These histograms show that the distribution of V_{Total} is highly skewed.

Summary statistics for the V_{Total} calculations are given in Table 4. Tables 5 and 6 list the maximum Category 1 and 5 wind speeds, respectively, at each vertex of the grid in Figure 1. Table 7 lists the maximum wind speeds for each of the 100 samples. This table shows that each category of hurricane has max wind speeds consistent with the Saffir-Simpson scale given in Table 8. However, as the frequencies in Table 7 show, not every combination of sample input represented by the LHS input vectors for Category 1 produces a maximum wind speed that meets the Saffir-Simpson scale for a Category 1 or a Category 5. This is to be expected as the ranges in Table 1 are consistent with the characteristics of Categories 1 or 5. However, not every possible combination of CP, Rmax, V_T, and FFP from the ranges in Table 1 guarantees a maximum wind speed consistent with the Saffir-Simpson scale for the respective storm category. Rather, the entire distribution of maximum winds speeds for either a Category 1 for Category 5 is consistent with maximum winds associated with that category via Saffir-Simpson.

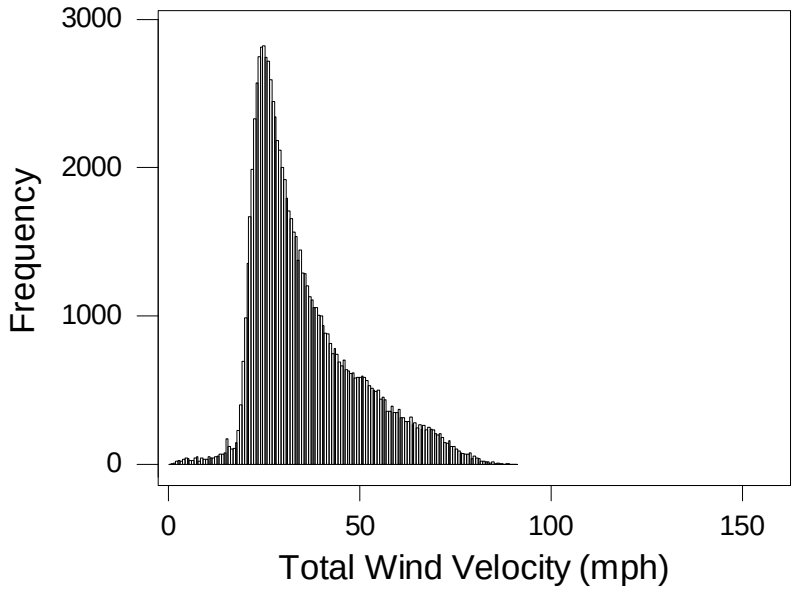

Figure 8. Histogram of Calculated V_{Total} Values for a Category 1 Hurricane

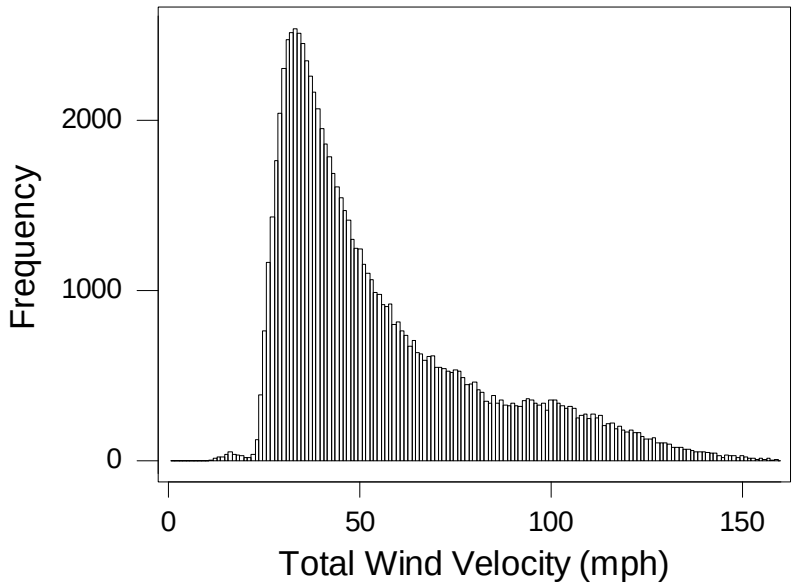

Figure 9. Histogram of Calculated V_{Total} Values for a Category 5 Hurricane

Table 4. Summary Statistics for V_{Total} Calculations by Hurricane Category

	Category 1	Category 5
Mean	36.0	54.9
Standard deviation	13.9	26.8
Median	31.8	45.6
Minimum	0.1	10.3
Maximum	91.1	164.5

Table 5. Maximum Wind Speed for Category 1 at Each Grid Vertex Defined in Table 1 (shaded cells indicated Category 1 wind speeds)

73.3	74.7	75.5	77.8	80.2	81.4	81.6	81.8	83.6	85.4	87.4	88.7	91.1	**15N**
71.6	75.2	71.7	71.3	73.1	75.2	76.7	78.6	80.8	84.2	85.2	86.0	83.6	**10N**
62.6	65.6	68.9	70.3	70.7	71.5	74.4	73.2	73.6	76.8	81.0	83.4	80.9	**5N**
58.1	60.3	62.5	66.6	65.9	68.3	68.9	69.3	71.0	74.8	76.3	78.2	75.3	**0**
53.1	55.8	57.1	59.1	62.2	63.3	65.4	64.6	66.2	69.0	72.5	75.2	71.7	**-5S**
180	**165**	**150**	**135**	**120**	**105**	**90**	**75**	**60**	**45**	**30**	**15**	**0**	

Table 6. Maximum Wind Speed for Category 5 at Each Grid Vertex Defined in Table 1 (shaded cells indicated Category 1 wind speeds)

116.7	114.8	115.6	118.4	123.9	127.7	129.1	129.0	131.5	133.8	136.1	138.2	140.3	**15N**
140.6	136.7	139.2	142.6	149.9	149.7	151.5	153.7	152.6	157.1	161.1	162.5	164.5	**10N**
131.7	134.6	143.5	141.0	143.2	144.1	145.1	148.8	155.4	151.1	155.3	150.3	149.1	**5N**
127.1	127.8	124.2	127.8	134.2	136.4	137.2	139.6	143.1	142.4	144.2	147.2	143.0	**0**
112.6	117.1	122.7	122.3	123.3	127.9	127.7	132.6	136.1	136.5	139.2	133.0	140.2	**-5S**
180	**165**	**150**	**135**	**120**	**105**	**90**	**75**	**60**	**45**	**30**	**15**	**0**	

Table 7. Frequency of Calculated Maximum Wind Speeds for the 100 LHS Input Vectors

Category 1		Category 5	
Max Wind Speed (mph)	**Frequency**	**Max Wind Speed (mph)**	**Frequency**
WS < 74	8	135 ≤ WS < 140	3
74 ≤ WS < 80	36	140 ≤ WS < 145	14
80 ≤ WS < 85	37	145 ≤ WS < 150	29
85 ≤ WS < 90	17	150 ≤ WS < 155	24
90 ≤ WS < 95	2	WS ≥ 155	30
Totals	100		100

Table 8. Saffir-Simpson Scale for Hurricane Intensity

Category	Speed (mph)	CP (mB)	Damage
1	74 ≤ WS < 96	≥ 980	Minimal
2	96 ≤ WS < 110	965 to 979	Moderate
3	110 ≤ WS < 130	945 to 964	Extensive
4	131 ≤ WS < 155	920 to 944	Extreme
5	WS ≥ 155	< 920	Catastrophic

Table 9. Sample Input Characteristics and V_{Total} for Category 5 at (30,0) for t = 1hr

Sample	CP	Rmax	V_T	FFP	V_{Total}
1	911.7	10.07	14.16	1013.4	112.0
2	909.1	7.64	18.15	1012.3	111.4
3	909.0	8.24	16.85	1012.3	110.4
…	**…**	**…**	**…**	**…**	**…**
100	907.9	7.82	14.42	1012.9	99.0

A very useful way to show wind patterns throughout the 5×13 grid is with a contour plot. Such a plot provides a view of the winds over the entire grid, much as a satellite image does. Contours of average wind speeds of 60mph, 80mph, 100mph, 120mph, and 140mph for a Category 5 hurricane are drawn throughout the grid for a given time. Figures 10 to 22 present contour plots from t = 0hr to t = 12hr, respectively.

As expected, these contour plots show the highest speed to the right of the path of the hurricane, which has a westerly heading. Moreover, the speed decreases as the hurricane moves over land. Decay was simulated in this demonstration analysis by assuming a 1mB and 3mB hourly increases in CP for Categories 1 and 5, respectively. Note the contour for 140mph disappears after 1hr, as does 120mph after 4hr and 100mph after 7hr.

Consideration now moves from the global view of the grid to focus on the behavior of V_{Total} at a single vertex in the grid at a given time. For example, Table 9 shows a portion of the sampled input characteristics in the LHS and the corresponding calculated value of V_{Total} for the Category 5 hurricane at coordinates (30,0) for t = 1hr. Since the LHS contains 100 different sets of input for the four parameters in Table 1, there will be 100 different values of V_{Total} calculated at each time. Moreover, there are 1300 calculated values of V_{Total} over all times at each vertex in the 5×13 grid. These values can be displayed in various ways to show the variability in V_{Total} at each time point.

One such display is given in Figure 23 where values of V_{Total} for a Category 5 at (30, 0) have been plotted as cumulative distribution functions (cdfs) for seven different times. This figure shows the highest winds at 1hr and 2hr. The greatest uncertainty (spread) occurs at 2hr (the actual range in wind speeds at 2hr was from 15mph to 144.2mph). The reason the range is so wide is that the eye of the storm is located at approximately (30, 0) at t = 2hr. The least uncertainty occurs at 12hr.

Figure 24 is similar to Figure 23, except the coordinates have been changed to (30, 10) which is 10mi to the right of the storm. Note the big difference in the cdfs in Figures 23 and 24 for t = 2 hr. Since the coordinates in Figure 24 are to the right of the eye of the storm, the wind speeds are not subject to the relative calmness associated with the eye and therefore do not have a wide range as was the case at (30, 0). Displays similar to Figure 23 could be made for any of the 65 vertices.

As stated previously, the goal of the sensitivity analysis is to determine the relative influence of CP, Rmax, V_T, and FFP on the magnitude of V_{Total} at each time while uncertainty analysis seeks to determine which of these input parameters contribute to the uncertainty in V_{Total} at each time. Methods for performing a sensitivity analysis will be presented first.

Two statistics will be considered as measures of the relative influence on the magnitude of V_{Total}: (1) partial correlation coefficients and (2) standardized regression coefficients. The calculation of the partial correlation coefficient is considered first. As is shown in the ensuing discussion, these two statistics are both derived from the inverse of the correlation matrix and are functionally related.

Partial Correlation Coefficients. Table 3 gave the actual pairwise correlations for the input parameters in Table 1 based on a LHS of size n=100 for Category 1 and Category 5. Table 10 is an extension of Table 3 to include the pairwise correlations of CP, Rmax, V_T, and FFP with V_{Total} at grid coordinates (30, 0) at t = 1hr. All calculations in Table 10 are based on Equation 1. The last row in the Category 5 portion of Table 10 shows CP, Rmax, V_T, and FFP have respective simple correlations of 0.187, 0.696, 0.675, and 0.066 with V_{Total}. To assist in interpreting these correlations, Figures 25 to 28 present scatterplots of wind speed versus CP, Rmax, V_T, and FFP, respectively. Note the indication of a strong relationship between wind speed and Rmax in Figure 25 and with V_T also in Figure 26. On the other hand, the scatterplots in Figures 25 and 28 indicate very weak relationships.

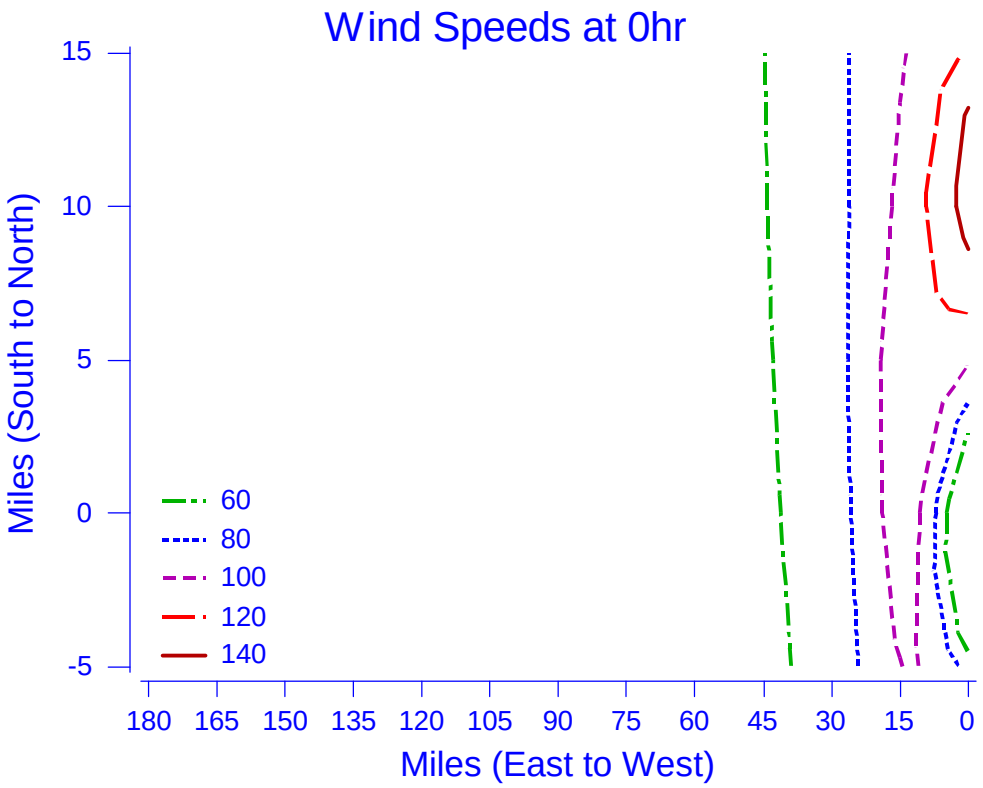

Figure 10. Contour Plot of Calculated Category 5 Wind Velocities at t = 0hr

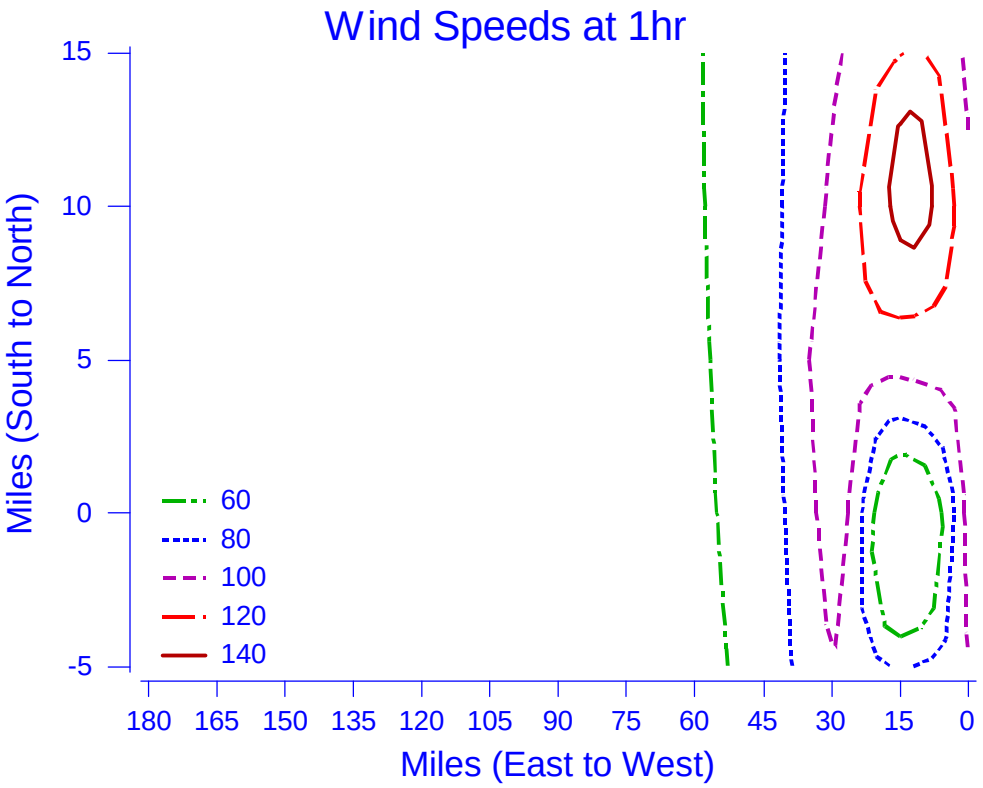

Figure 11. Contour Plot of Calculated Category 5 Wind Velocities at t = 1hr

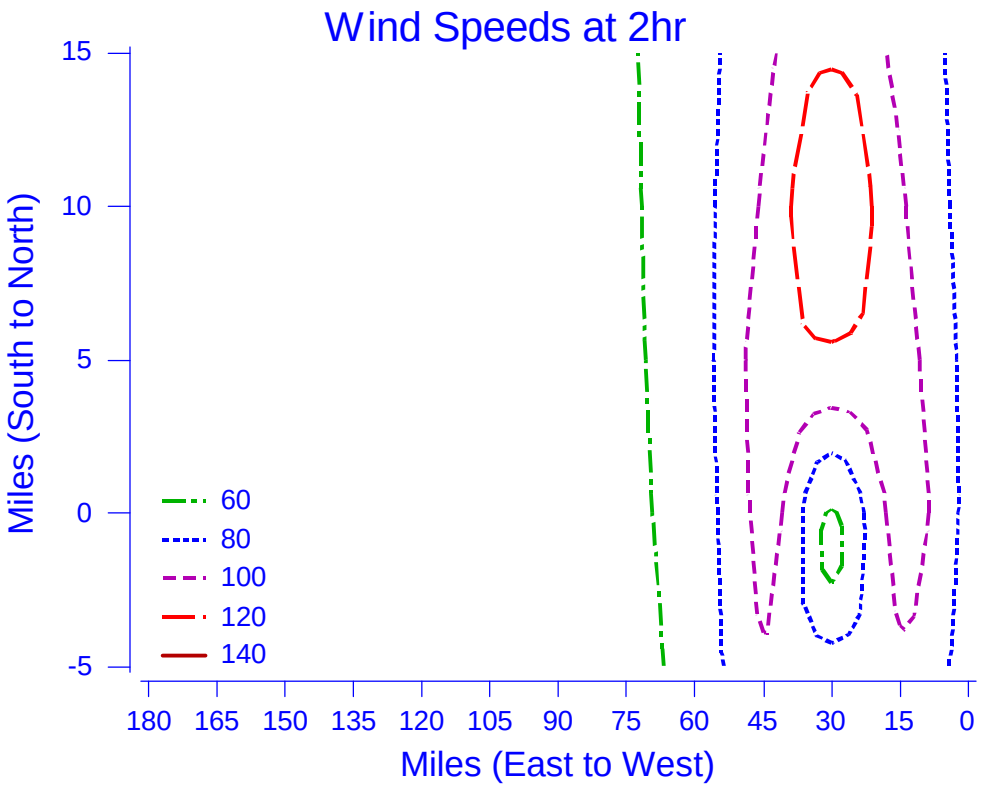

Figure 12. Contour Plot of Calculated Category 5 Wind Velocities at t = 2hr

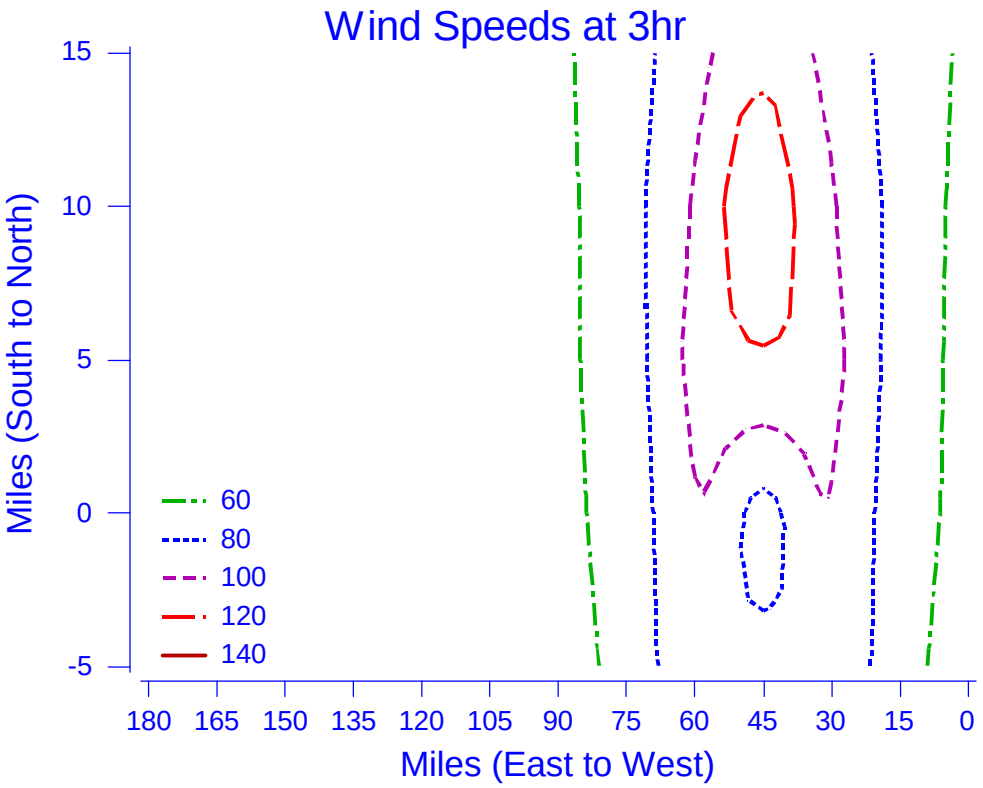

Figure 13. Contour Plot of Calculated Category 5 Wind Velocities at t = 3hr

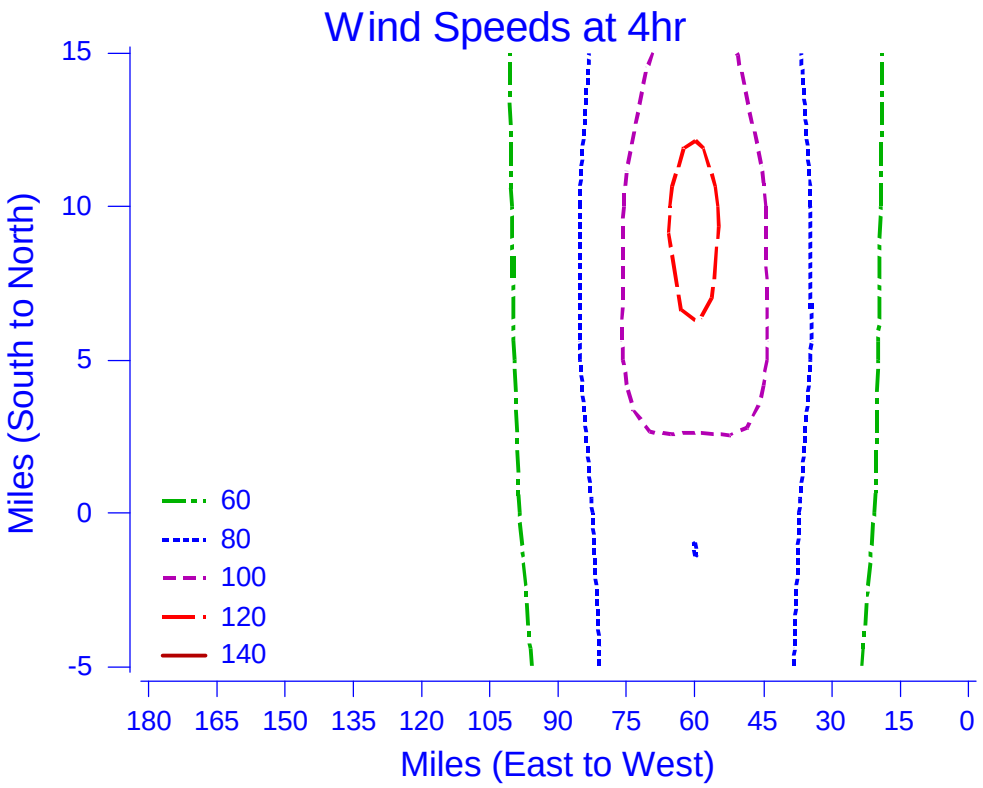

Figure 14. Contour Plot of Calculated Category 5 Wind Velocities at t = 4hr

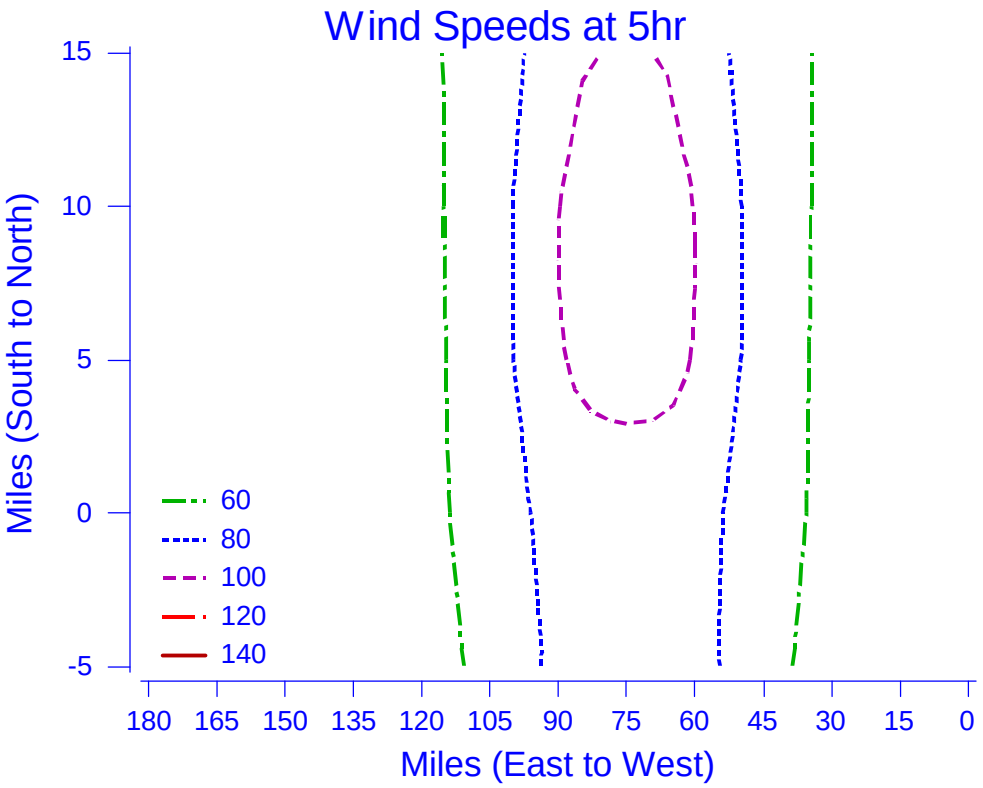

Figure 15. Contour Plot of Calculated Category 5 Wind Velocities at t = 5hr

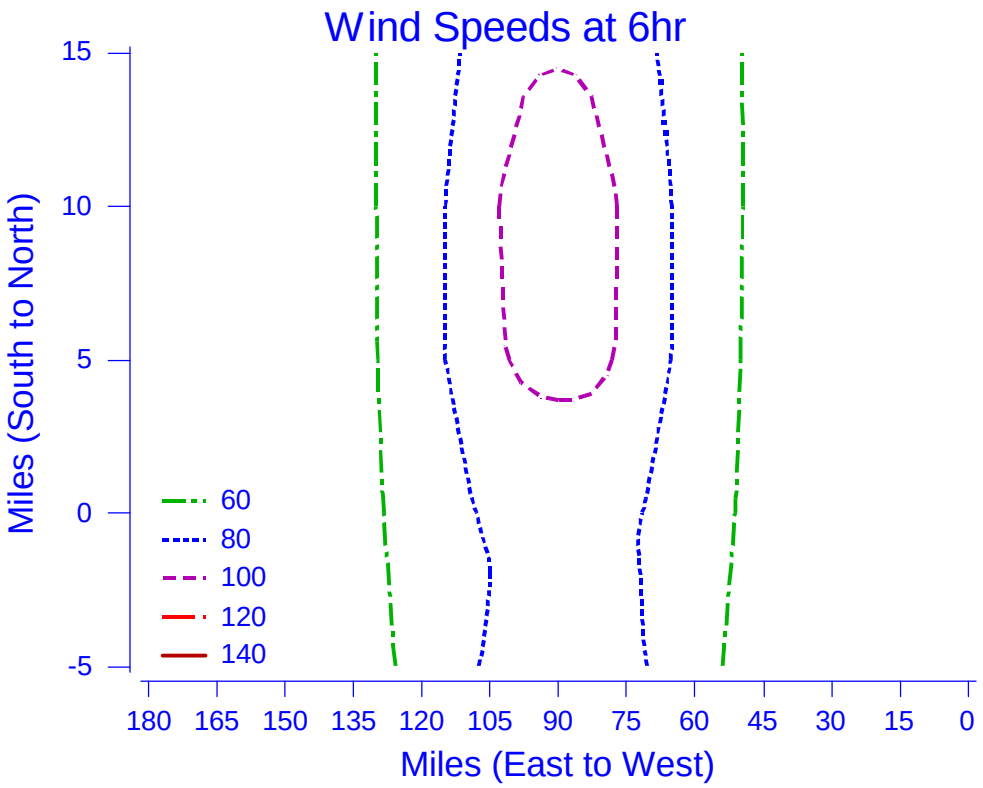

Figure 16. Contour Plot of Calculated Category 5 Wind Velocities at t = 6hr

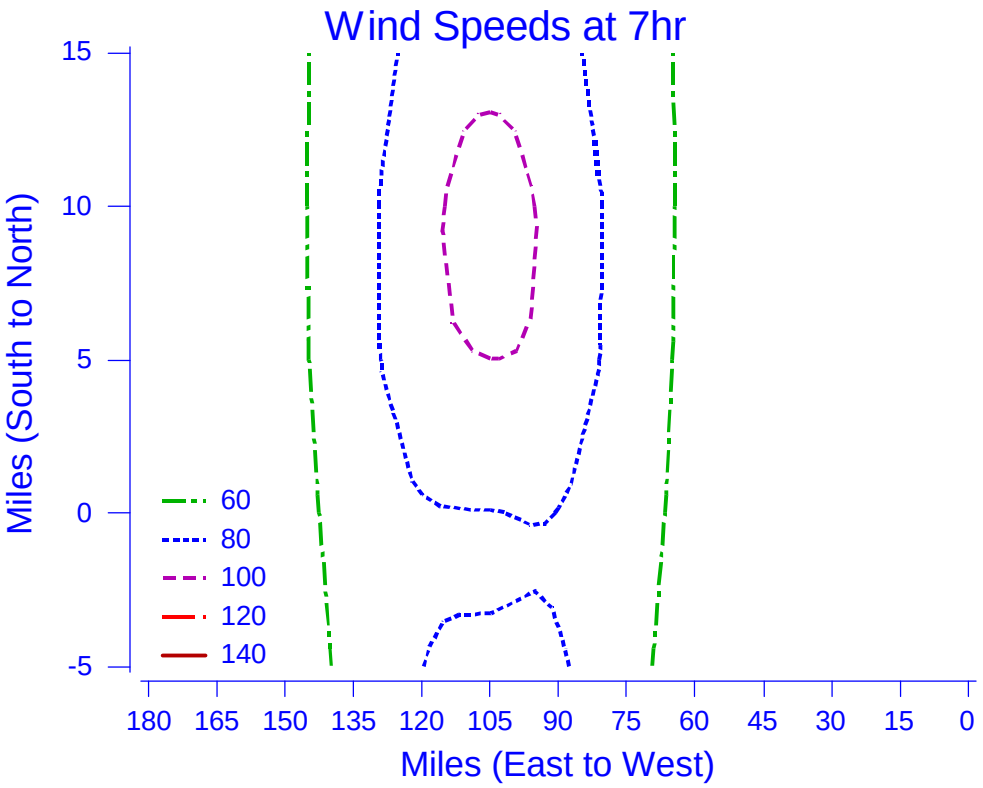

Figure 17. Contour Plot of Calculated Category 5 Wind Velocities at t = 7hr

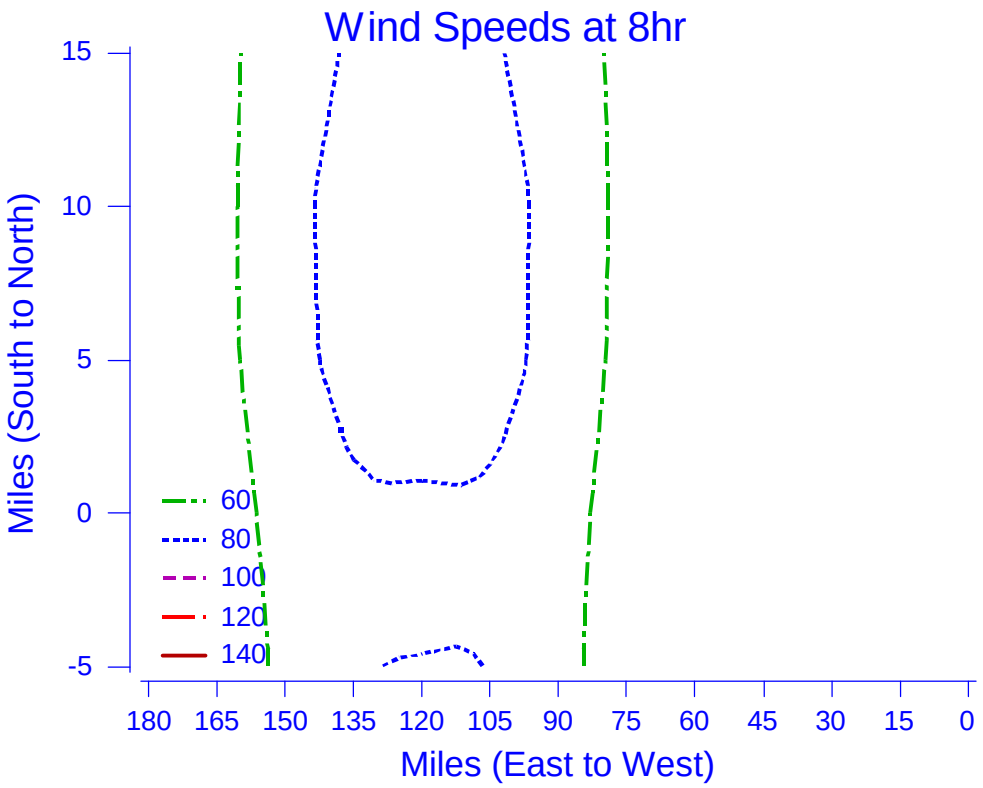

Figure 18. Contour Plot of Calculated Category 5 Wind Velocities at t = 8hr

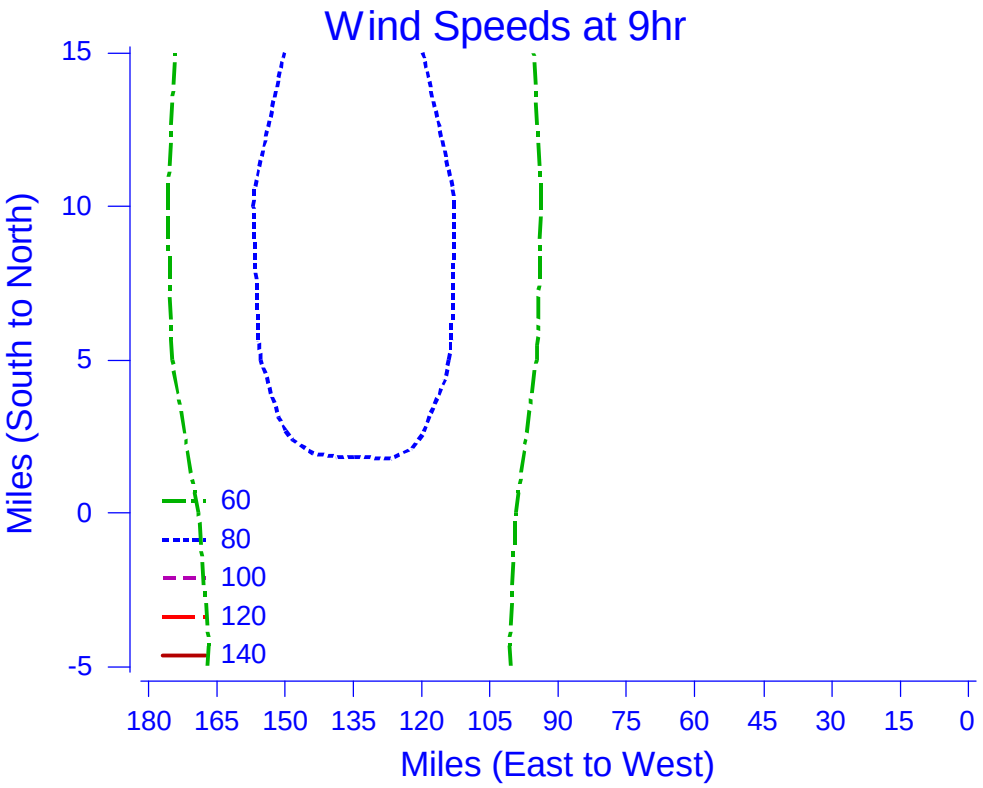

Figure 19. Contour Plot of Calculated Category 5 Wind Velocities at t = 9hr

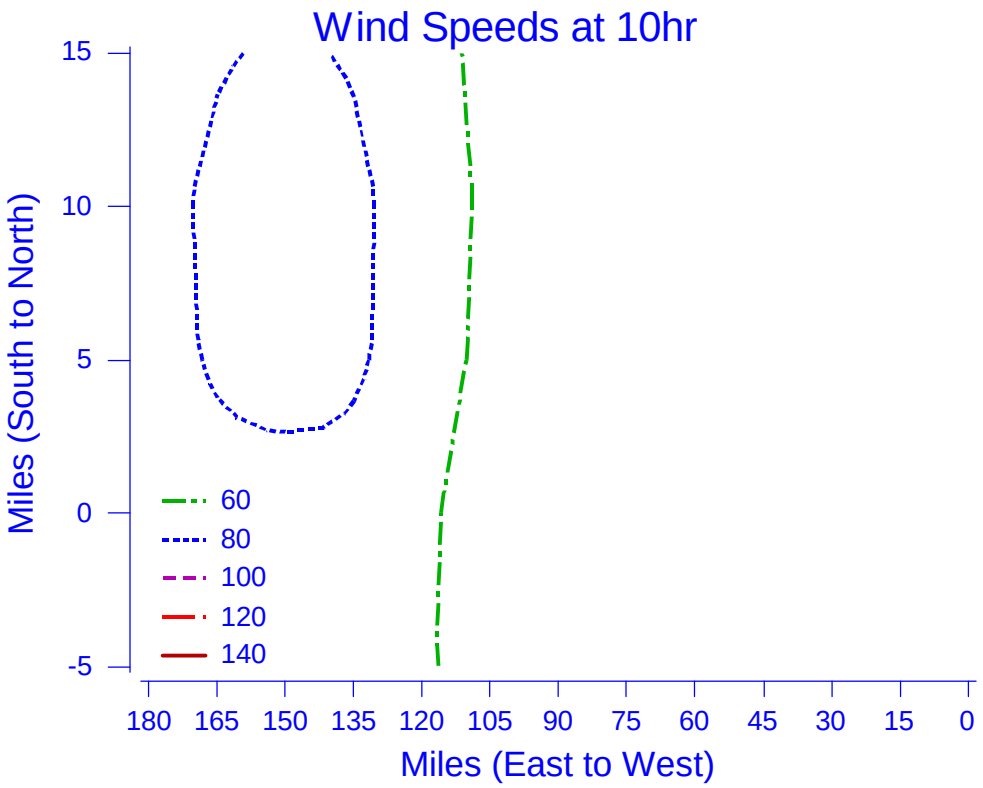

Figure 20. Contour Plot of Calculated Category 5 Wind Velocities at t = 10hr

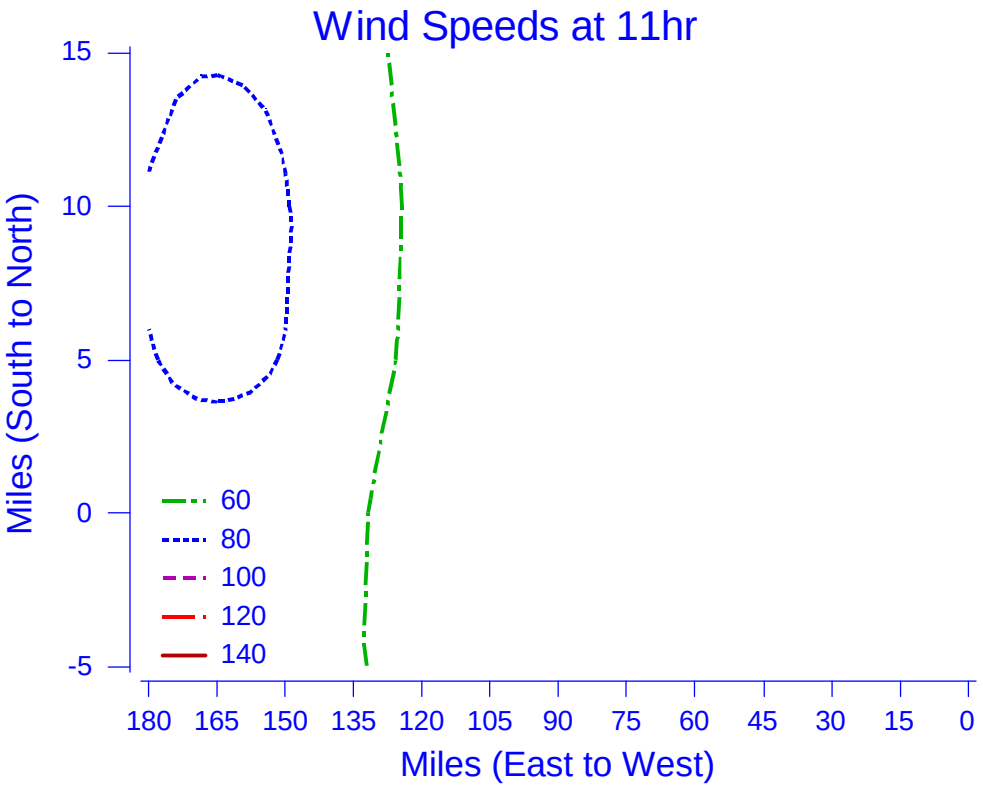

Figure 21. Contour Plot of Calculated Category 5 Wind Velocities at t = 11hr

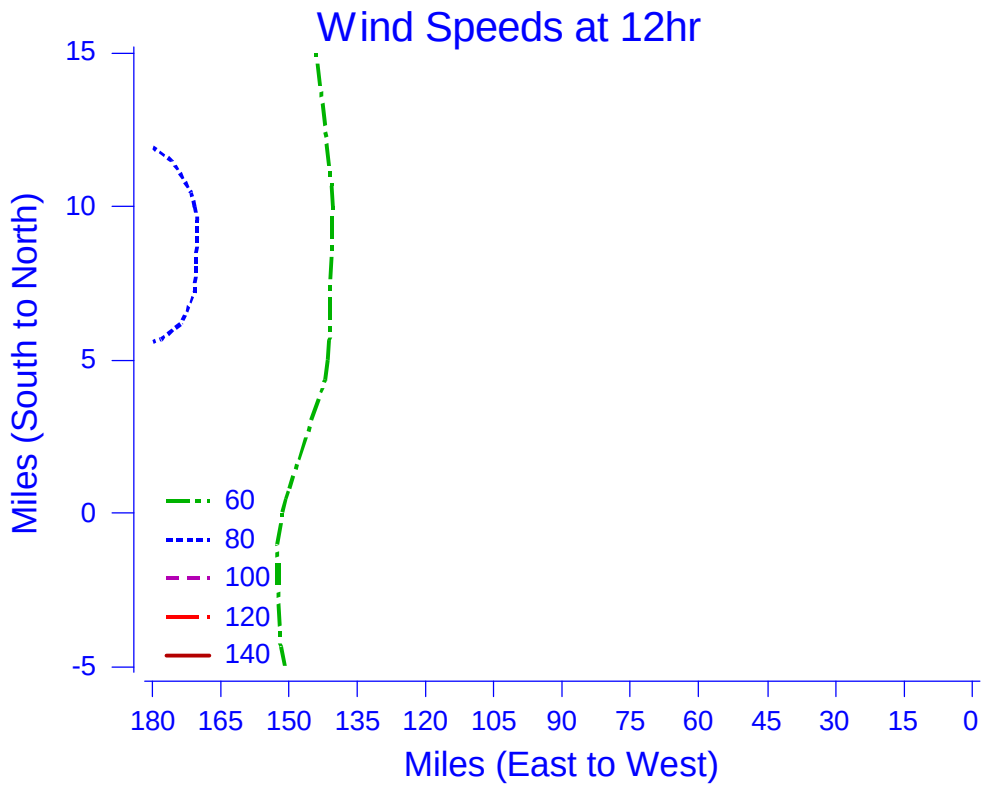

Figure 22. Contour Plot of Calculated Category 5 Wind Velocities at t = 12hr

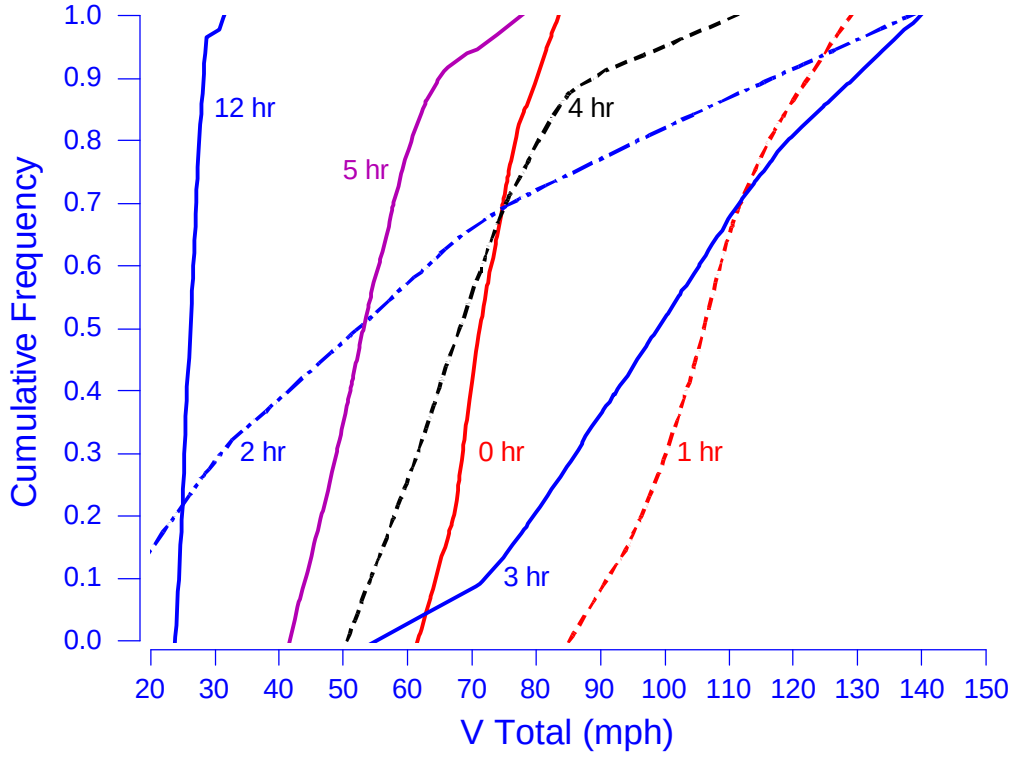

Figure 23. Cumulative Distributions for V_{Total} at Coordinates (30, 0) for a Category 5 at Various Times

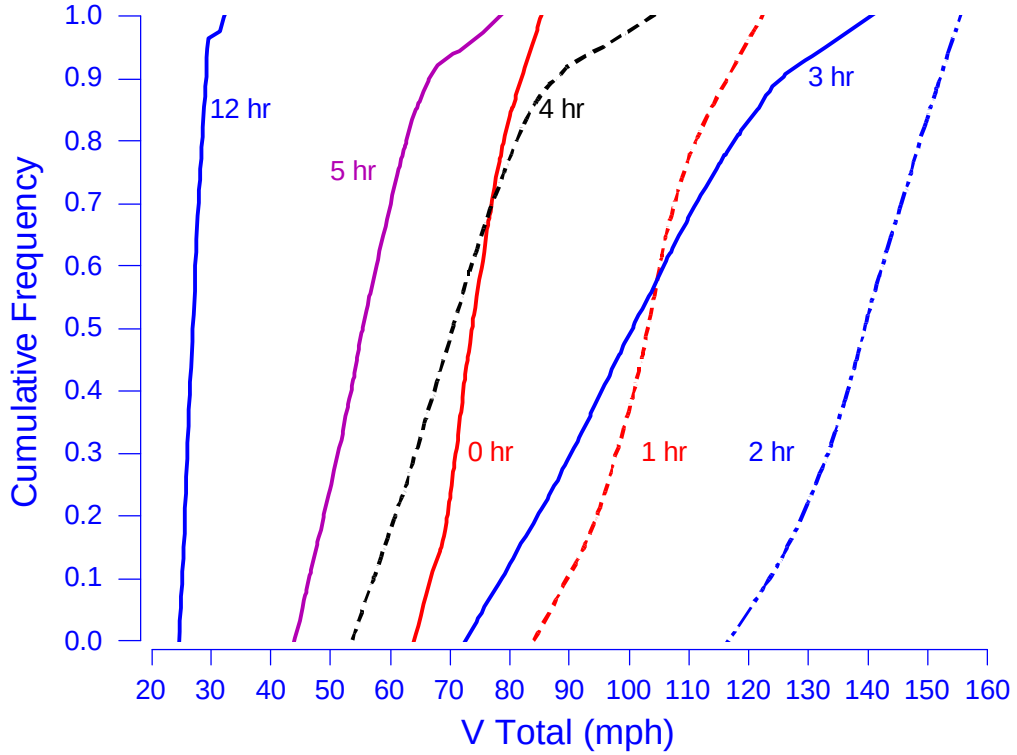

Figure 24. Cumulative Distributions for V_{Total} at Coordinates (30, 10) for a Category 5 at Various Times

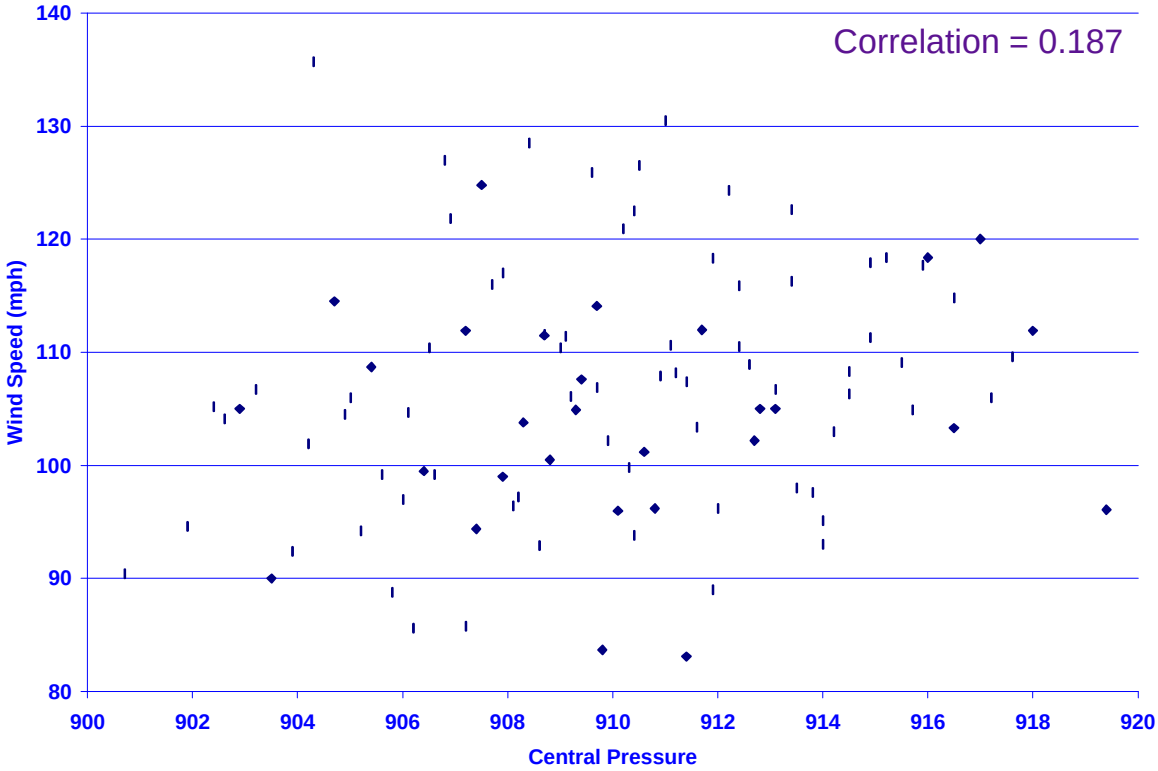

Figure 25. Scatterplot of Wind Speed vs CP at (30, 0) for a Category 5 at t = 1hr

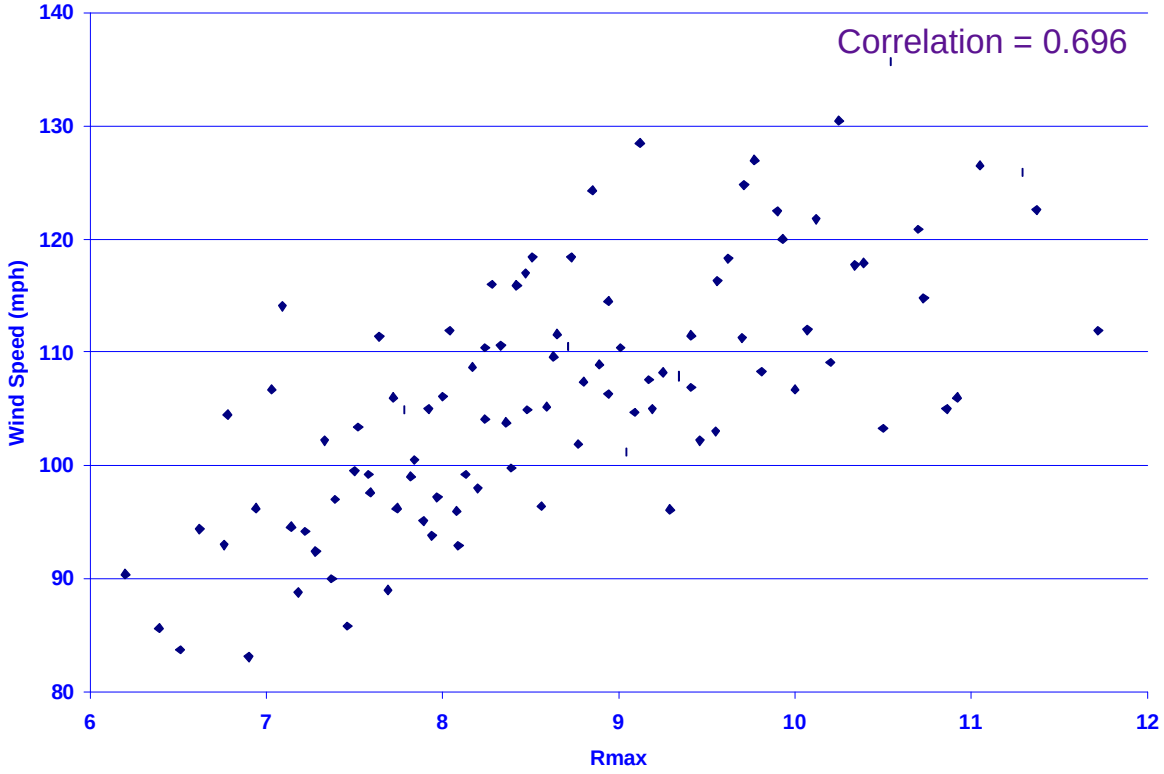

Figure 26. Scatterplot of Wind Speed vs Rmax at (30, 0) for a Category 5 at t = 1hr

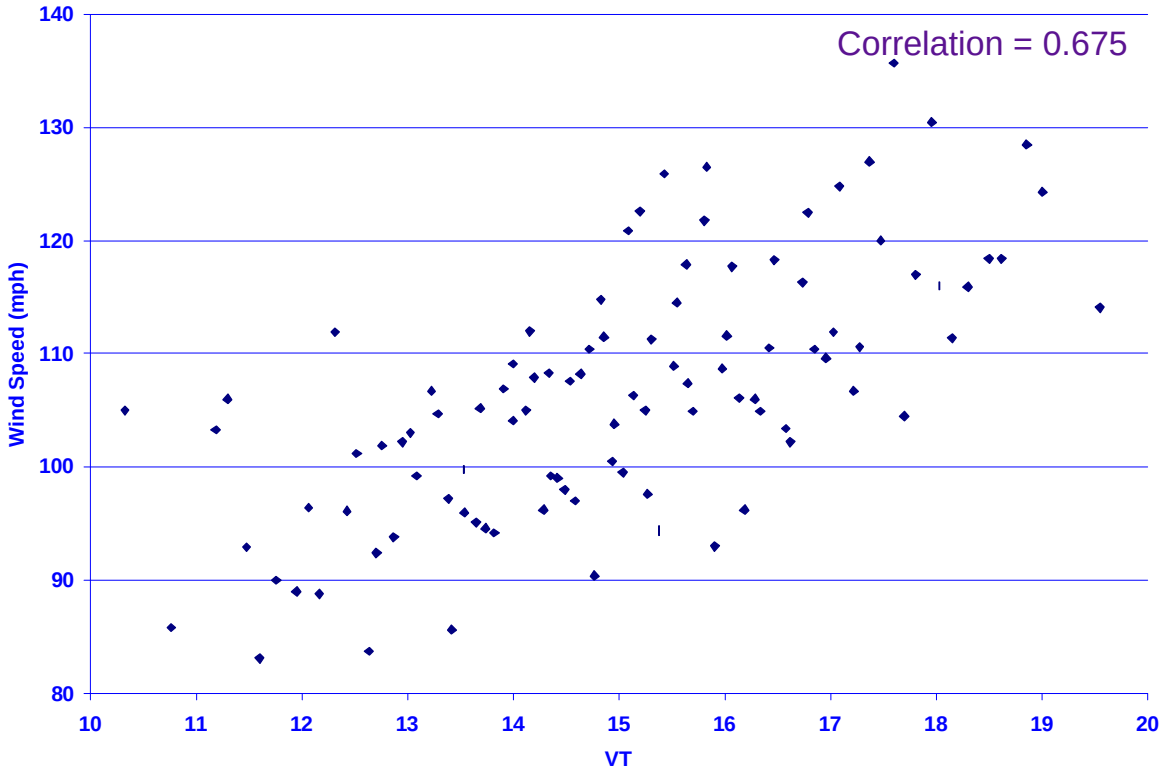

Figure 27. Scatterplot of Wind Speed vs V_T at (30, 0) for a Category 5 at t = 1hr

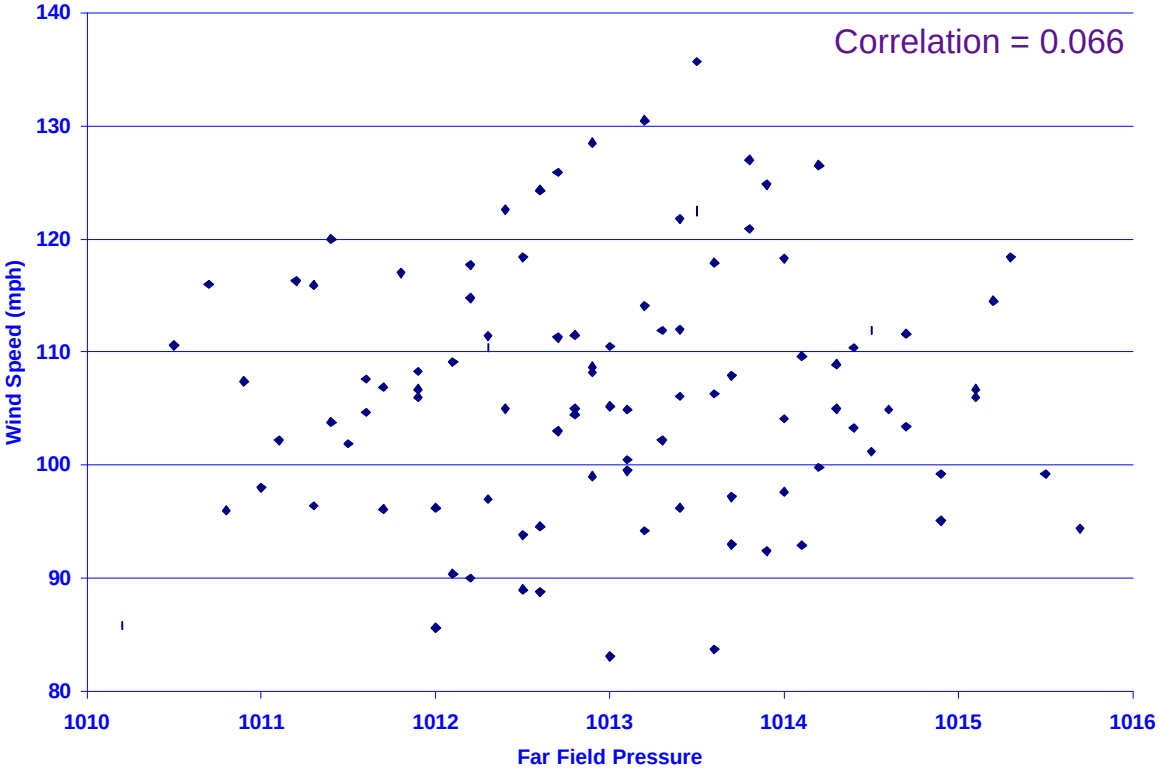

Figure 28. Scatterplot of Wind Speed vs FFP at (30, 0) for a Category 5 at t = 1hr

Table 10. Simple Correlations among CP, Rmax, V_T, and FFP and V_{Total} for the Category 1 and Category 5 Analysis at Grid Coordinate (30, 0) at t = 1hr

	Category 1					Category 5				
CP	1.000	0.250	0.006	-0.007	-0.400	1.000	0.490	-0.006	0.007	0.187
Rmax	0.250	1.000	-0.013	0.025	-0.377	0.490	1.000	-0.012	-0.013	0.696
V_T	0.006	-0.013	1.000	0.007	-0.602	-0.006	-0.012	1.000	-0.007	0.675
FFP	-0.007	0.025	0.007	1.000	0.260	0.007	-0.013	-0.007	1.000	0.066
V_{Total}	-0.400	-0.377	-0.602	0.260	1.000	0.187	0.696	0.675	0.066	1.000
	CP	**Rmax**	**V_T**	**FFP**	**V_{Total}**	**CP**	**Rmax**	**V_T**	**FFP**	**V_{Total}**

Rmax and V_T have the highest simple correlation with V_{Total} in Table 10, which might lead one to believe that these two parameters have the most influence on V_{Total}. That may indeed turn out to be true, but the answer is not as straightforward as the simple correlations might lead one to believe since Cp and Rmax are also correlated with each other. It is necessary to determine what correlation remains between Cp and V_{Total} after their respective correlations with Rmax are accounted for. The measure that is used to provide the needed information is *partial correlation*.

Partial correlation differs from simple correlation in that it measures the degree of linear relationship between a given input parameter in Table 1 (denoted as X_j) and the wind velocity (denoted as Y) following an adjustment to remove the linear effect of the other three input parameters. Partial correlations coefficients (PCC) were calculated for each input parameter in Table 1 at each of the 65 vertices in the 5×13 grid at each time point (t = 0, 1, 2, …, 12hr) as a measure of their relative influence on the magnitude of V_{Total}. The calculation of these partial correlations is now considered in detail.

One of the more efficient ways of calculating PCCs is based on the inverse of the simple correlation matrix **C**. The inverse of the correlation matrix **C** is denoted by $\mathbf{C}^{-1}$. The product of **C** and $\mathbf{C}^{-1}$ is the identity matrix (a matrix with

$$\mathbf{C}^{-1} = \begin{bmatrix} 1/\left(1-R_{x_1}^2\right) & c_{12} & c_{13} & c_{14} & -b_1/\left(1-R_y^2\right) \\ c_{21} & 1/\left(1-R_{x_2}^2\right) & c_{23} & c_{24} & -b_2/\left(1-R_y^2\right) \\ c_{31} & c_{32} & 1/\left(1-R_{x_3}^2\right) & c_{34} & -b_3/\left(1-R_y^2\right) \\ c_{41} & c_{42} & c_{43} & 1/\left(1-R_{x_4}^2\right) & -b_4/\left(1-R_y^2\right) \\ -b_1/\left(1-R_y^2\right) & -b_2/\left(1-R_y^2\right) & -b_3/\left(1-R_y^2\right) & -b_4/\left(1-R_y^2\right) & 1/\left(1-R_y^2\right) \end{bmatrix}$$

Figure 29. General Form of the Inverse of a Correlation Matrix

ones along the main diagonal from the upper left-hand corner to the lower right-hand corner with zeros elsewhere). The inverse of a correlation matrix **C** is shown in general terms in Figure 29.

The PCC for X_j and Y is obtained directly from $\mathbf{C}^{-1}$ as

$$PCC_{x_j y} = -c_{jy} \Big/ \sqrt{c_{jj} c_{yy}} \tag{9}$$

Example 1. The inverse of the correlation matrix in Table 10 is given in Table 11. Using Equation 9 with Table 11, the PCCs are found as follows:

Table 11. Inverse of the Category 5 Correlation Matrix Given In Table 10

CP	5.4212	-16.3256	-13.3241	-0.97613	19.4112
Rmax	-16.3256	61.2154	50.8599	3.79309	-74.1506
V_T	-13.3241	50.8599	44.1520	3.23023	-62.9367
FFP	-0.9761	3.7931	3.2302	1.24326	-4.7206
$\mathbf{V_{Total}}$	19.4112	-74.1506	-62.9367	-4.72062	91.7931
	CP	**Rmax**	$\mathbf{V_T}$	**FFP**	$\mathbf{V_{Total}}$

The PCC for CP and V_{Total} is found from Equation 9 as:

$$PCC_{CP,V_{Total}} = \frac{-19.4112}{\sqrt{(5.4212)(91.7931)}} = -0.871$$

Likewise, the PCC for Rmax and V_{Total} is found as:

$$PCC_{R\max,V_{Total}} = \frac{-(-74.1506)}{\sqrt{(61.2154)(91.7931)}} = 0.989$$

The PCC for V_T and V_{Total} is found as:

$$PCC_{V_T,V_{Total}} = \frac{-(-62.9367)}{\sqrt{(44.1520)(91.7931)}} = 0.989$$

Finally, the PCC for FFP and V_{Total} is found as:

$$PCC_{FFP,V_{Total}} = \frac{-(-4.72062)}{\sqrt{(1.24326)(91.7931)}} = 0.448$$

Parameters with partial correlations close to 0 have very little, if any, influence on the magnitude of the model output response. The above calculations indicate that FFP has the least relative influence on V_{Total}. Parameters with PCCs close to 1 have a strong positive effect on the model output response. In this example, Rmax and V_T have nearly identical PCCs that are very close to 1, indicating that V_{Total} increases as these parameters increase. On the other hand, parameters with PCCs correlations close to -1 have a strong negative effect on the model output response, which means that V_{Total} will decrease as these parameters increase. Such is the case with CP, which has a strong negative partial correlation close to -1. Overall, Rmax and V_T have the most effect on the magnitude of V_{Total} at coordinates (30, 0) with t = 1hr. Next in order is CP followed by FFP. The corresponding PCC calculations for Category 1 were: -0.473, -0.469, -0.729, and 0.425.

Standardized Regression Coefficients. A model that regresses V_{Total} on CP, Rmax, V_T, and FFP could be fit at each vertex in the 5×13 grid for each time point. Such a model would have the following form:

$$V_{Total} = \beta_0 + \beta_1 CP + \beta_2 Rmax + \beta_3 V_T + \beta_4 FFP \qquad (10)$$

where the coefficients $\beta_0, \ldots, \beta_4$ are determined by least squares calculations. It would be tempting to use these coefficients as measures of relative influence, i.e. large values have lots of influence and small values have very little influence. The fallacy in this suggestion lies in the fact that the coefficients reflect the units for each parameter: CP and FFP are measured in mB while Rmax and V_T are measured in miles and mph, respectively.

This does not imply that the regression approach is without merit as the units dilemma is easily resolved by using standardized regression coefficients (SRC), which permit comparison of the coefficients in common or standardized units. The value b_j in $\mathbf{C}^{-1}$ in Figure 29 is the standardized regression coefficient for X_j corresponding to the regression model in Equation 10. The value R^2_y is the percentage of variation in Y explained by the regression on X_1, X_2, X_3, and X_4. The value R^2_{xj} is the coefficient of determination from regressing X_j on Y and the remaining Xs.

Example 2. The SRCs are found from Table 11 by multiplying the reciprocal of the element in the lower right-hand corner of $\mathbf{C}^{-1}$ (91.7931) times the first four elements in the last row of $\mathbf{C}^{-1}$ as follows:

The SRC for CP is found:

$$SRC_{CP} = \frac{-19.4112}{91.7931} = -0.212$$

Likewise, the SRC for Rmax is found as:

$$SRC_{R\max} = \frac{-(-74.1506)}{91.7931} = 0.808$$

The SRC V_T is found as:

$$SRC_{V_T} = \frac{-(-62.9367)}{91.7931} = 0.686$$

Finally, the SRC for FFP is found as:

$$SRC_{FFP} = \frac{-(-4.72062)}{91.7931} = 0.052$$

Parameters with SRCs close to 0 have very little, if any, influence on the magnitude of the model output response. The above calculations indicate that FFP with a SRC = 0.052 has the least influence on V_{Total}. Parameters with positive SRCs have a positive effect on the model output response. In this example, Rmax has the highest positive SRC followed by V_T. Note that while the PCCs for these two parameters were identical, the SRCs differ somewhat. As with PCCs, parameters with negative SRCs have a negative effect on the model output response. The SRC for CP = -0.212 indicates that CP has a negative effect on V_{Total}. Overall, Rmax and V_T have the most effect on the magnitude of V_{Total} at coordinates (30, 0) with t = 1hr. Next in order is CP followed by FFP. Note that this ordering

is in agreement with the results for PCCs. This is not just happenstance, as the PCC and SRC are functionally related as shown in the following equation.

Using Equation 9 and the elements in the last row of $\mathbf{C}^{-1}$, the PCC can be written as

$$PCC_{x_j y} = \frac{-(-b_j)/\left(1-R_y^2\right)}{\sqrt{\left(\frac{1}{1-R_{x_j}^2}\right)\left(\frac{1}{1-R_y^2}\right)}} = b_j\sqrt{\frac{1-R_{x_j}^2}{1-R_y^2}} \tag{11}$$

This shows the functional relationship between PCC and SRC (denoted as b_j in Equation 11). The corresponding SRC calculations for Category 1 were: -0.315, -0.312, -0.605, and 0.267.

Table 12. Summary of the Influence of the Four Input Parameters as Measured by SRCs at Coordinate (30, 0) over the 12hr Time Period

	Category 1	Category 5
CP	• Maximum influence at t=0hr and later hrs • Almost no influence at t=2hr when the eye of the storm is at (30, 0) • Increasing negative influence for t ≥ 3hr	• Maximum influence at t=0hr • Almost no influence at t=2hr when the eye of the storm is at (30, 0) • Nearly constant for t ≥ 4hr with a slight negative influence — less than for Category 1
Rmax	• Maximum influence at t=0hr • Switches to negative at t=1hr and 2hr as the eye of the storm is at (30, 0) • Increasing strong positive influence for t > 3hr	• Maximum influence at t=0hr • Strong positive at t=1hr • Switches to slightly negative as the eye of the storm is at (30, 0) • Increasing strong positive influence for t > 2hr
V_T	• Slightly negative influence at t=0hr • Strong negative influence at t=1hr • No influence at t=2hr as the hurricane approaches (30, 0) • Strong positive influence at t=3hr • Switches to a strong negative influence for t=4hr and then gradually increases to no influence at t=11hr and finishes slightly positive	• No influence on at t=0hr • Strong positive influence at 1hr as the hurricane approaches (30, 0) • No influence at t=2hr • Switches to a strong negative influence after the storm passes by (30, 0)
FFP	• Positive influence at t=0hr • No influence at t=1hr and then gradually increases in influence over the remainder of the 12hr time period	• FFP is nearly constant throughout the 12hr time period and has very little influence

Display of Sensitivity Measures versus Time. While Examples 1 and 2 utilized only one time period at a single grid point, it is very much of interest to see how the influence of CP, Rmax, V_T, and FFP relative to V_{Total} changes over time. Figures 30 and 31 show respective plots of the Category 1 and 5 SRCs for each of the four input parameters at coordinates (30, 0) for t = 0hr, 1hr, …, 12hr.

The changing nature of the curves in Figures 30 and 31 makes it very clear why the temporal aspect of V_{Total} must be considered when performing a sensitivity analysis. While the SRCs plotted in Figures 25 and 26 at t = 1hr match those calculated in Example 2, these values change dramatically at t = 2hr when the eye of the storm is very close to being centered at the coordinates (30, 0) that were used in Example 2. The relative influence of each of the four input parameters at (30, 0) versus time is summarized in Table 12.

Appendix B contains five complete sets of graphs similar to Figures 30 and 31 for the following coordinates:

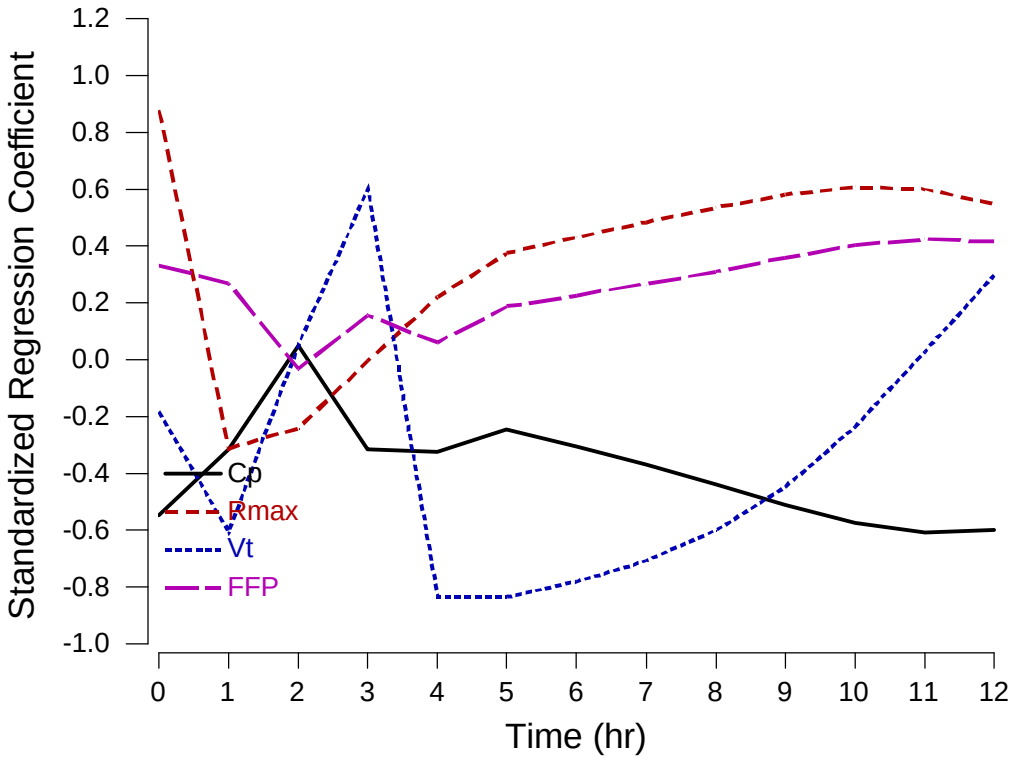

Figure 30. Standardized Regression Coefficients vs. time at Grid Coordinates (30, 0) for Category 1

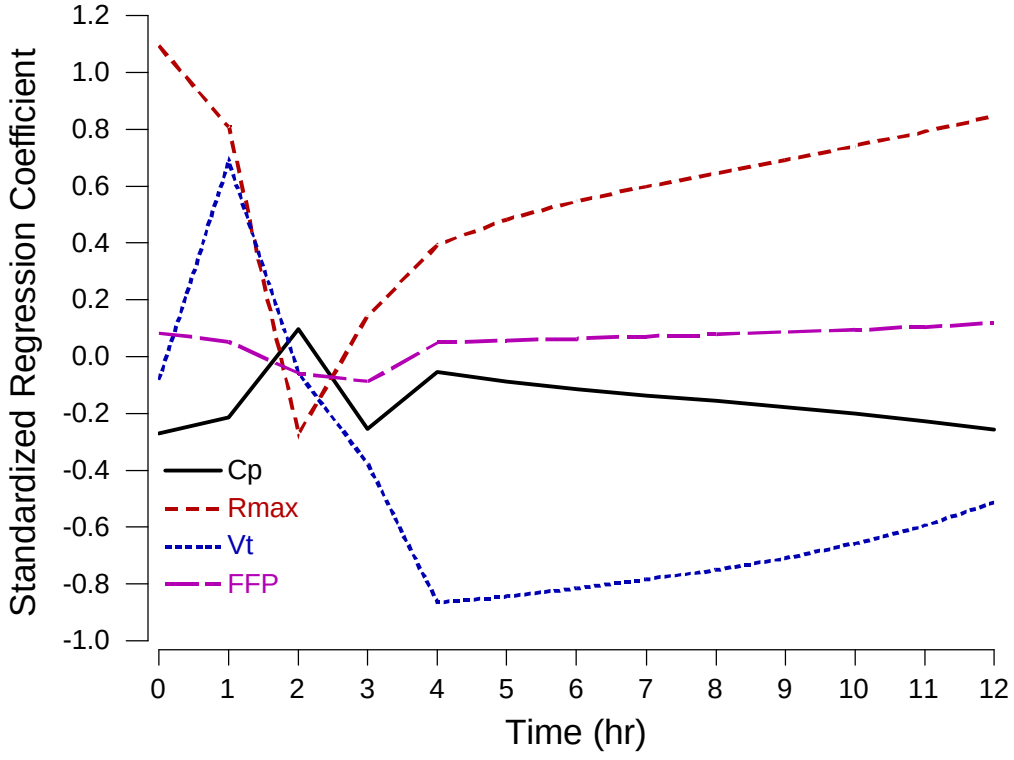

Figure 31. Standardized Regression Coefficients vs. time at Grid Coordinates (30, 0) for Category 5

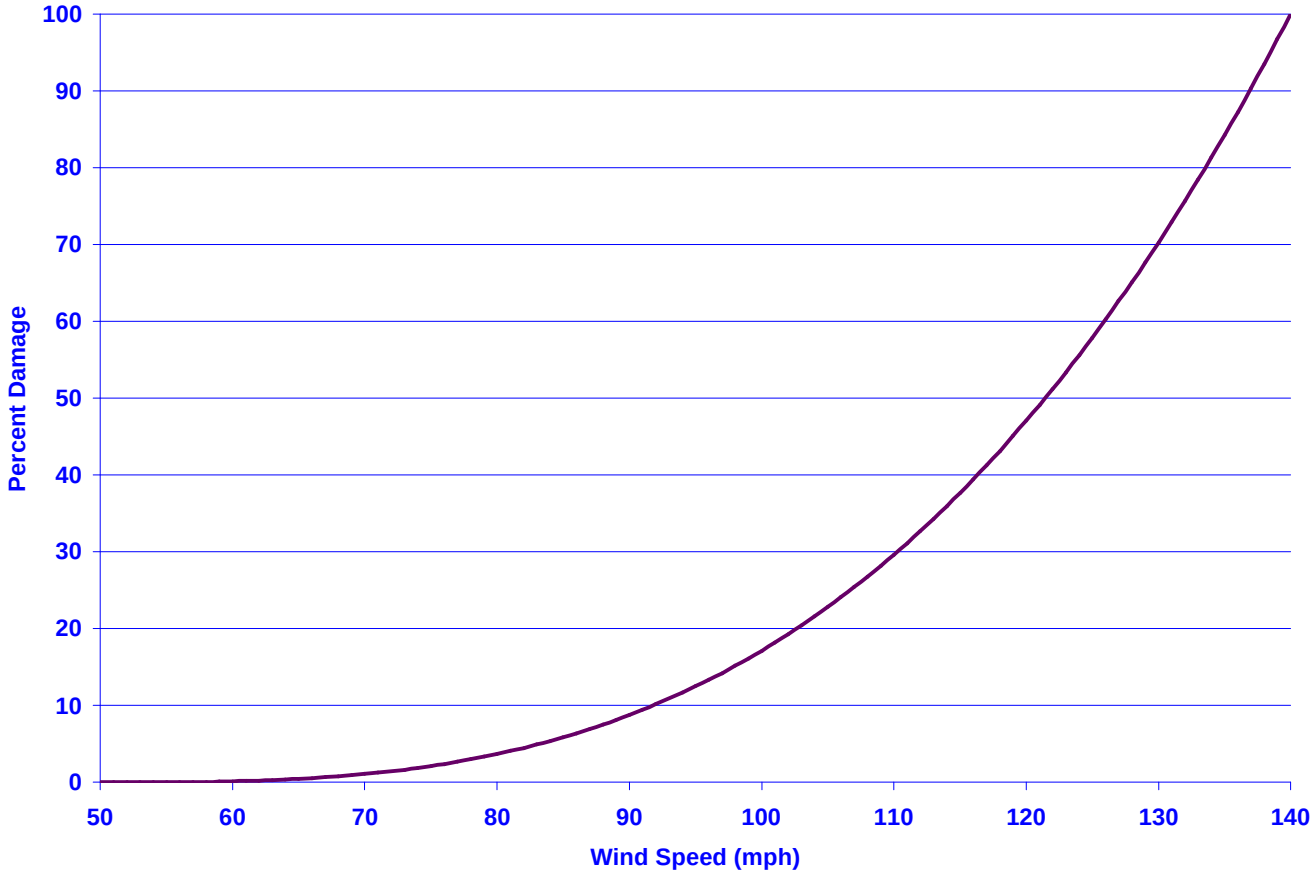

Figure 32. Surrogate Damage Function Used in Demonstration Analysis

- 5mi south of the path of the eye: (0, -5) to (180, -5)
- Path of the eye: (0, 0) to (180, 0)
- 5mi north of the path of the eye: (0, 5) to (180, 5)
- 10mi north of the path of the eye: (0, 10) to (180, 10)
- 15mi north of the path of the eye: (0, 15) to (180, 15)

Conversion to Loss Cost. The analyses to this point have demonstrated sensitivity analyses for calculated V_{Total} values utilizing the four input characteristics presented in Table 1. Specifically, the goal of these analyses was to show the impact of CP, Rmax, V_T, and FFP on V_{Total}. In this section, V_{Total} is converted to loss cost using a simple lost cost function to see how the sensitivity analysis results change with the output variable.

Assume there is a $100,000 structure at each vertex in the grid with a 1% or $1000 deductible. For simplicity, assume this applies to all vertices whose X coordinate is ≥ 15mi, as hurricane monitoring commenced 15mi offshore. Apply the following cubic damage function to convert V_{Total} to percentage damage:

$$\%Damage = \left(\frac{V_{Total} - 50}{140 - 50} \right)^3 \tag{12}$$

This surrogate damage function appears in graphical form in Figure 32.

Note that this expression is a surrogate for an actual, operational damage function. The intent is not to use a function that meets FCHLPM standards, but rather acts in the place of such a function to illustrate the techniques and reveal the types of graphical and numerical analyses possible with the approach.

The loss cost function is developed from the damage function in Equation 12 as follows:

1. If %Damage is ≤ 1%, total loss = \$0. This corresponds to $V_{Total} \leq 69.39$mph.
2. If %Damage is ≥ 50%, total loss = \$99,000. This corresponds to $V_{Total} \geq 121.43$mph.
3. Otherwise, total loss = %Damage × \$100,000 - \$1,000

Loss costs can be summed at a fixed time t over all vertices with X ≥ 15mi (i.e. 60 vertices) to get total loss cost at time t. Moreover, sensitivity analyses could be performed to determine the influence of the four input parameters in Table 1 on hourly loss costs in the same manner that was just illustrated for V_{Total}. However, hourly loss costs are of limited utility since the maximum total loss cost during the 12hr period is the statistic of primary interest.

Maximum total cost is simply the highest loss incurred during the 12hr (assuming no duration effects). Since each of the n=100 LHS input vectors has an associated maximum total loss cost, the sensitivity analysis is performed on this statistic as the response variable corresponding to each of the n=100 sets of LHS input characteristics. Figures 33 and 34 show these n=100 responses as estimated cumulative distribution functions for total loss cost for Category 1 and 5, respectively. Figure 35 presents a contour plot of total loss cost for Category 5.

Table 13. SRCs for Total Loss Cost by Category of Hurricane

	Category 1				Category 5			
	CP	**Rmax**	**V_T**	**FFP**	**CP**	**Rmax**	**V_T**	**FFP**
SRC	-0.759	-0.026	0.017	0.441	-0.614	0.887	0.076	0.147
Rank	1	3	4	2	2	1	4	3

The SRCs for the maximum total loss cost are found following the procedures outline in Example 2. Table 13 gives the SRCs and their corresponding ranks from 1 (most influential SRC) to 4 (least influential SRC). Note that CP and FFP are most influential for Category 1 while Rmax and CP are most influential for Category 5.

One final comment to close the discussion of SA for total loss cost is now provided. The previous SA for V_{Total} focused on individual vertices at individual time points t = 0hr to 12hr. As such, the four input parameters were directly related to V_{Total} through the Rankine-vortex function and the SA identified these relationships. On the other hand, the SA results for total loss cost do not focus on individual wind speeds at a given vertex at a given time point. Rather, much information is folded together prior to performing the SA. To explain, the loss cost function greatly changed the nature of the relationship between the input parameters and the output by setting any wind speed ≤ 69.39mph to \$0 and any speed ≥ 121.43mph to \$99,000. Next, an additional level of folding of the data occurs when only the maximum loss cost over the 12hr period is used. Obviously, this maximum occurs at different times for different combinations of input parameters in the LHS. A final level of folding occurs when these maxima are summed over the entire grid. Hence, the SA results for total loss cost require careful interpretation. On the other hand, temporal variation of potential damage and loss is probably subordinate to the estimated total losses.

Uncertainty Analysis. As stated in the Introduction, the goal of uncertainty analysis is to quantify the contributions of the input parameters to the uncertainty in V_{Total}. This goal is frequently *misinterpreted* as meaning a quantification of the uncertainty in V_{Total} or the development of confidence intervals about the mean or distribution function for V_{Total}. An extended simple example is used to convey the goal of uncertainty analysis. Consider the following simple model:

$$Y = X_1 + X_2 + X_3 + X_4 \tag{13}$$

These X's have associated uncertainties that are characterized with uniform distributions in the same sense as was done for the input parameters in Table 2 with triangular distributions. Specifically, X_1 is distributed uniformly on the interval from 0 to 1, which is denoted as $X_1 \sim U(0, 1)$. Similarly, $X_2 \sim U(0, 2)$, $X_3 \sim U(0, 3)$ and $X_4 \sim U(0, 4)$. The expected (mean) value of a random variable X with a uniform distribution on the interval (a, b) is given as:

$$E(X) = \frac{a+b}{2} \tag{14}$$

and the variance is found as

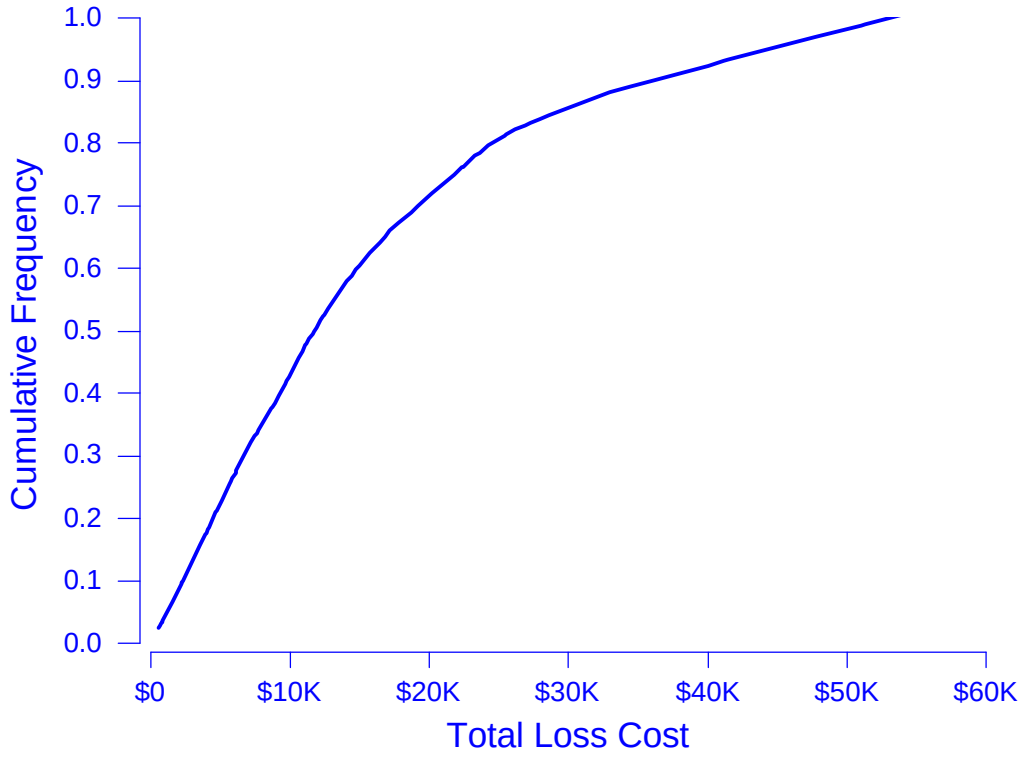

Figure 33. Distribution of Total Loss Cost for a Category 1 Hurricane

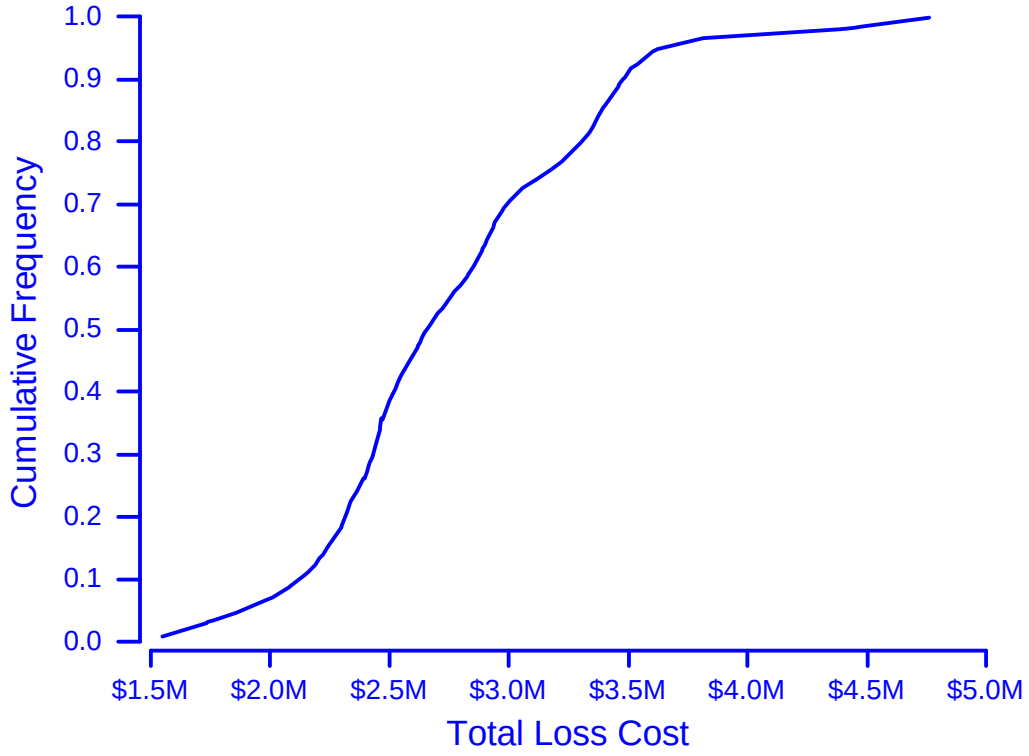

Figure 34. Distribution of Total Loss Cost for a Category 5 Hurricane

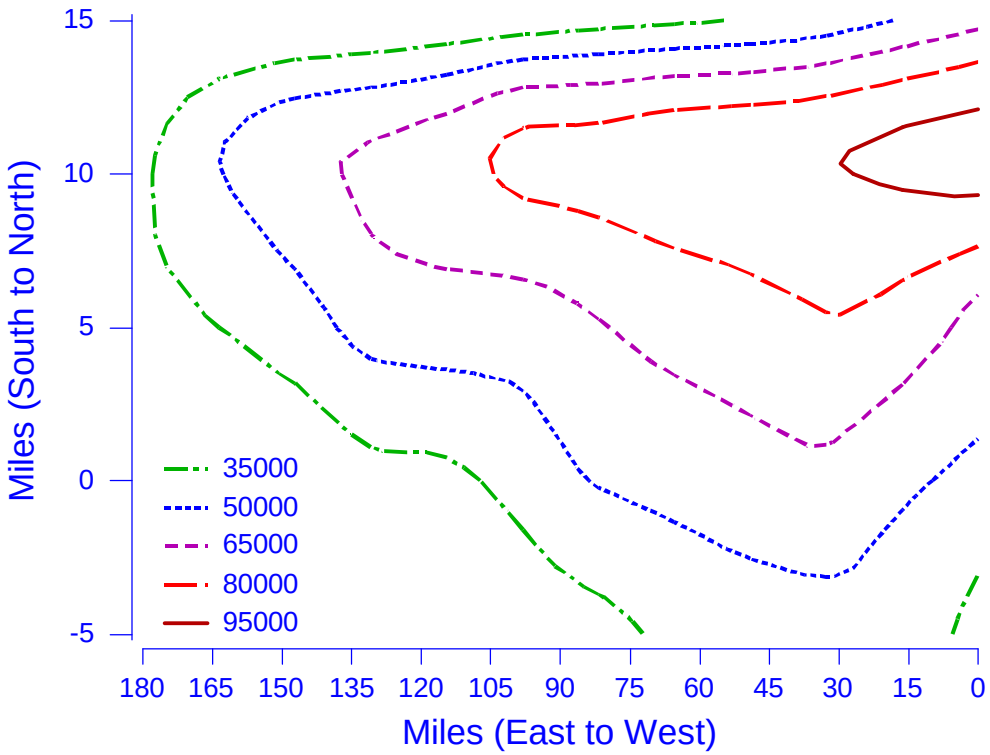

Figure 35. Distribution of Total Loss Cost for a Category 5 Hurricane

$$V(X) = \frac{(b-a)^2}{12} \tag{15}$$

Applying Equations 14 and 15 to X_1, X_2, X_3, and X_4 yields the following means and variances:

	E(X)	V(X)
X_1	0.5	1/12
X_2	1.0	4/12
X_3	1.5	9/12
X_4	2.0	16/12

The mean or expected value of Y is found directly from these values and Equation 13 as

$$E(Y) = E(X_1) + E(X_2) + E(X_3) + E(X_4) \tag{16}$$

or

$$E(Y) = 0.5 + 1.0 + 1.5 + 2.0 = 5.0$$

Likewise, the variance of Y is found as

$$V(Y) = V(X_1) + V(X_2) + V(X_3) + V(X_4) \tag{17}$$

or

$$V(Y) = (1/12) + (4/12) + (9/12) + (16/12) = 30/12 = 2.50$$

This latter value is a measure of the variability in Y, which could also be expressed in terms of the standard deviation, 1.58.

When Y is a function of the values of X, such as given in Equation 13, there is a well known result in mathematical statistics (e.g. Parzen, 1962) whereby the unconditional variance of a random variable can be expressed in terms of the conditional variance as follows:

$$Var(Y) = E_{X_j}\left[Var(Y \mid X_j)\right] + Var_{X_j}\left[E(Y \mid X_j)\right] \tag{18}$$

In words, the variance of Y is equal to the mean of the conditional variance plus the variance of the conditional mean. The first term on the right-hand side of Equation 18 is the expected value of the variance of Y taken over the variable X_j. If Equation 18 is rewritten as

$$Var(Y) - E_{X_j}\left[Var(Y \mid X_j)\right] = Var_{X_j}\left[E(Y \mid X_j)\right] \tag{19}$$

then the right-hand side represents the expected reduction in the variance of Y due to ascertaining the value of X_j. The contribution to the uncertainty in Y attributable to X_j or the expected percentage reduction in V(Y) due to knowing X_j is given in Iman (1987) as:

$$\text{Expected percentage reduction in Var(Y)} = \frac{Var\left(E\left[Y \mid X_j\right]\right)}{Var(Y)} \times 100\% \tag{20}$$

Since the exact functional form of the simple model and its inputs are known in this simple example, the answer to the uncertainty question is straightforward. Equation 20 gives the following expected percentage reductions in the V(Y) for X_1 to X_4 using the above variances:

Input Parameter	Expected Percentage Reduction when the Input Parameter is Known
X_1	(1/12)/(30/12)×100% = 3.3%
X_2	(4/12)/(30/12)×100% = 13.3%
X_3	(9/12)/(30/12)×100% = 30.0%
X_4	(16/12)/(30/12)×100% = 53.3%

Thus, the expected reduction in the V(Y) is only 3.3% if the value of X_1 is known with certainty, but the expected reduction in the V(Y) for X_4 is 53.3%. If the goal is to reduce the variability in Y, then the biggest payoff is associated with a reduction in the variability in X_4. That is, research dollars invested in better knowledge of X_4 has great potential to reduce the uncertainty in Y than do any of the other input parameters. Note that these results have nothing to do with confidence intervals for the variability in Y, which as mentioned previously, is a frequent misinterpretation of uncertainty analysis.

Uncertainty Analysis Results for V_{Total}. Actual computer models are greatly removed from the simplicity of the model in Equation 13, so methods have to be devised to estimate the expected percentage reduction from Equation 20 based on actual computer input and output. One such method given in Iman (1987) is now outlined. Iman refers to this measure as uncertainty importance.

Step 1. The variance of the output Y (such as V_{Total}) from a hurricane model (i.e. the denominator of Equation 18) is estimated from *n* computer runs using randomly selected values of the input parameters. In particular, let **X** represent an $n \times 4$ matrix of sample input characteristics to be utilized with the computer model. In the current analysis for V_{Total}, the number of computer runs is n=100.

$$X = \begin{bmatrix} X_{1,1} & X_{1,2} & X_{1,3} & X_{1,4} \\ X_{2,1} & X_{2,2} & X_{2,3} & X_{2,4} \\ & \vdots & & \\ X_{n,1} & X_{n,2} & X_{n,3} & X_{n,4} \end{bmatrix} \tag{21}$$

The first run of the model is based on the sample inputs in the first row of **X**, the second run utilizes the sample

inputs in the second row of **X**, and so on until the n^{th} run uses the sample inputs in the last or n^{th} row of **X**.

Step 2. Let $\mathbf{X}_M$ represent a vector of means of the four input parameters:

$$X_M = \left[\overline{X}_1 \quad \overline{X}_2 \quad \overline{X}_3 \quad \overline{X}_4\right] \tag{22}$$

Note: these means are usually estimated from sample inputs in the columns of the matrix **X**.

Step 3. Generate a new matrix of inputs $\mathbf{X_1}^*$ by replacing the last three entries in each row of **X** with their corresponding means from the vector $\mathbf{X}_M$ given in Equation 22. The new matrix appears as follows:

$$X_1^* = \begin{bmatrix} X_{1,1} & \overline{X}_2 & \overline{X}_3 & \overline{X}_4 \\ X_{2,1} & \overline{X}_2 & \overline{X}_3 & \overline{X}_4 \\ & \vdots & & \\ X_{n,1} & \overline{X}_2 & \overline{X}_3 & \overline{X}_4 \end{bmatrix} \tag{23}$$

Step 4. Run the model using the matrix $\mathbf{X_1}^*$ in Equation 23 and calculate V(Y). Denote this variance as $V(E[Y|X_1])$, which is the numerator in Equation 20.

Step 5. Repeat steps 3 and 4 for X_2 where the 1st, 3rd, and 4th columns of **X** are replaced by their respective means in the vector $\mathbf{X}_M$. Denote the resulting variance estimate as $V(E[Y|X_2])$.

Step 6. Repeat steps 3 and 4 for X_3 where the 1st, 2nd, and 4th columns of **X** are replaced by their respective means in the vector $\mathbf{X}_M$. Denote the resulting variance estimate as $V(E[Y|X_3])$.

Step 7. Repeat steps 3 and 4 for X_4 where the 1st, 2nd, and 3rd columns of **X** are replaced by their respective means in the vector $\mathbf{X}_M$. Denote the resulting variance estimate as $V(E[Y|X_4])$.

Step 8. Substitute the estimates in Steps 4-7 into Equation 20 with the estimate of V(Y) from Step 1 to estimate the expected percentage reductions for X_1 to X_4.

These steps are now illustrated using the simple model in Equation 13. Random samples of size n=100 were obtained for each of the X's based on their respective uniform distributions. Hence the **X** matrix has 100 rows and 4 columns. The resultant simulated mean for Y was 4.87 with a variance of 2.163. The respective variance estimates in Steps 4 to 7 were: 0.093, 0.316, 0.805, and 1.108. The expected percentage reductions are found by substituting these values into Equation 18 as follows.

Parameter	$V(E[Y\|X_i])$ / V(Y)*100%	True Value
X_1	(0.093)/(2.163)×100% = 4.3%	3.3%
X_2	(0.316)/(2.163)×100% = 14.6%	13.3%
X_3	(0.805)/(2.163)×100% = 37.2%	30.0%
X_4	(1.108)/(2.163)×100% = 51.2%	53.3%

These estimates are reasonably close to the true values and improve with increased values of n as illustrated in the following results for n = 1,000 and n = 10,000.

Parameter	***n*=100**	***n*=1,000**	***n*=10,000**	True Value
X_1	4.3%	3.5%	3.3%	3.3%
X_2	14.6%	13.2%	13.2%	13.3%
X_3	37.2%	31.3%	29.7%	30.0%
X_4	51.2%	55.6%	52.9%	53.3%

Uncertainty analysis for V_{Total} is obviously more involved than this simple example since an UA can be performed at each of the 13 time points for each of the 65 vertices in the grid ($13 \times 65 = 845$ analyses). Moreover, the Rankine-vortex function for calculating V_{Total} is considerably more complicated than the simple model in Equation 13.

As was the case with sensitivity analysis, it is very much of interest to see how CP, Rmax, V_T, and FFP influence the uncertainty in V_{Total} over time. Figures 36 to 49 show plots of the expected percentage reductions in the variance of V_{Total} for Category 1 and 5 hurricanes for each of the four input parameters at the following pairs of coordinates along the path of the eye of the hurricane: (0, 0), (15, 0), (30, 0), (45, 0), (60, 0), (75, 0) and (180, 0).

Figures 36 and 37 show that V_T is the only contributor to uncertainty in V_{Total} at (0, 0) at t = 0hr. This result is correct as the eye of the hurricane is at (0, 0) at t = 0hr so that only V_T impacts V_{Total}. At t = 1hr, the eye has moved west of (0, 0) and the influence of V_T is greatly reduced while Rmax becomes a significant contributor to the uncertainty in V_{Total}. This result is also consistent with the physical reality. V_T is an important contributor to the uncertainty during the remaining times for a Category 1 hurricane as its influence decreases and then increases. V_T is also an important contributor to the uncertainty for a Category 5 hurricane, but has decreasing influence during the later stages of storm progression.

The contribution of Rmax increases when the contribution of V_T decreases and vice versa for both Category 1 and Category 5 (see comments accompanying Equation 24). The contribution of CP to the uncertainty in V_{Total} at (0, 0) for Category 1 gradually increases and actually surpasses that of V_T at t = 6hr before starting to decrease at t = 9hr. The contribution CP increases over time for a Category 5 but is much less than for a Category 1. FFP makes a significant contribution to the uncertainty in V_{Total} at (0, 0) throughout the 12hr period for a Category 1. The contribution of FFP increases throughout the 12hr period for a Category 5, but is much less than for a Category 1.

Unlike the result in Figures 36 and 37, where V_T was the only contributor to uncertainty at t = 0hr, Figures 38 and 39 show that Rmax is the main contributor to uncertainty at (15, 0) at t = 0hr. This is reasonable since (15, 0) is directly west of the eye of the hurricane at t = 0hr. At t = 1hr, the eye has moved to approximately (15, 0) and the results are similar to those in Figures 36 and 37 at t = 0hr, with V_T being the only contributor to the uncertainty in V_{Total}. The relative contributions for $t \geq 2$hr are similar to those in Figures 36 and 37 with the exception that the magnitude of the contribution from V_T has increased while the contribution of Rmax has decreased.

One interesting result occurs in Figure 39 where the contribution from V_T at t = 0hr is 118.7%. The interpretation of this result is that the uncertainty in V_{Total} actually increases based on the 8-step calculation procedure outlined above. Recall that the sample means were used in Step 2 and 3 as shown in Equations 22 and 23. The calculations for expected percentage reduction are sensitive to the type of statistic used in these steps. For example, rather than using the means in Equation 22, the minimums or maximums could be used. Use of these values would certainly change the relative contributions on the four input parameters. In fact, use of the minimums and maximums is one possible way of bounding the range of the contributions to uncertainty.

Figures 40 to 49 show that the general patterns of Figures 38 and 39 continue with the relative contributions of V_T and Rmax determined by the position of the grid vertex relative to the position of the eye at time t.

As mentioned above, the graphs in Figures 36 to 49 appear to exhibit a tradeoff pattern similar to what one might expect in a zero sum game. That is, the sum of the four contributions at any time is close to 100%. This pattern is more apparent for the Category 5 graphs where the roles of V_T and Rmax appear to be acting in concert. The reason for this behavior is that the wind speeds produced by the Rankine-vortex model are very closely approximated by the following simple linear model:

$$V_{Total} = \beta_0 + \beta_1 CP + \beta_2 Rmax + \beta_3 V_T + \beta_4 FFP \qquad (24)$$

This model explains the following percentage of variation in V_{Total} at (30, 0) for each value of t.

0hr	1hr	2hr	3hr	4hr	5hr	6hr	7hr	8hr	9hr	10 hr	11hr	12hr
99.6%	98.8%	4.2%	25.5%	92.1%	94.4%	95.1%	95.2%	95.2%	95.0%	94.8%	94.4%	94.2%

Since the percentages are so high, except when the eye of the storm is close to (30, 0), the sum of the contributions to the variation in V_{Total} will be very close to 100%, which explains the "zero-sum" patterns in Figures 36 to 49.

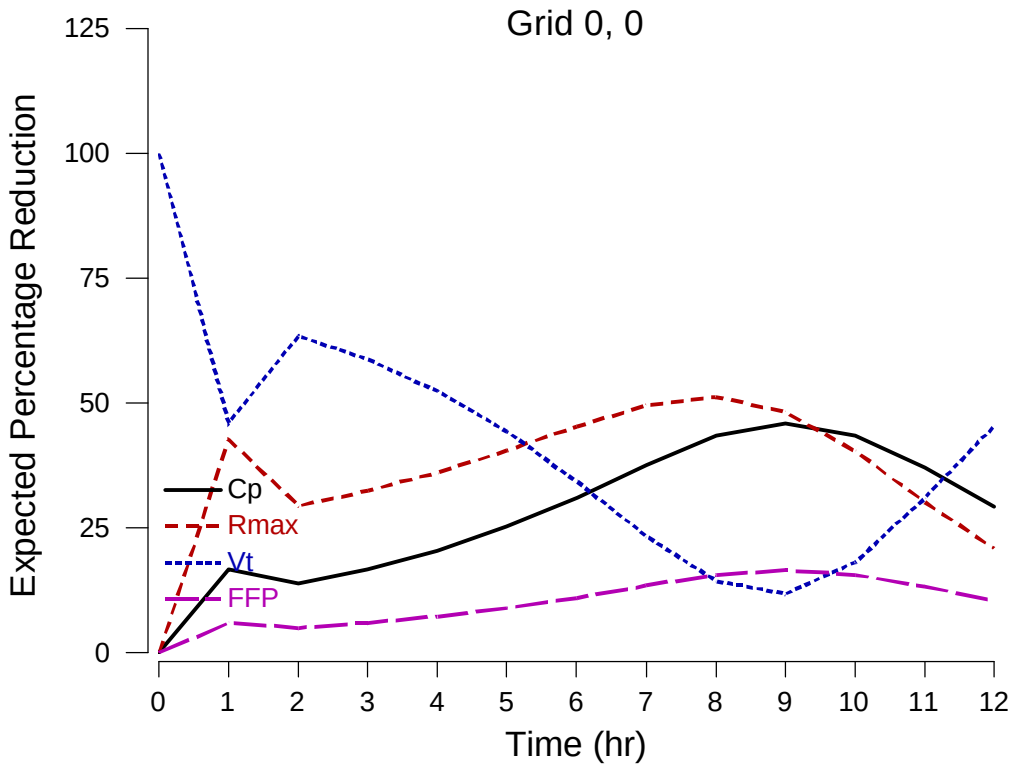

Figure 36. Expected Percentage Reductions in the Var(V_{Total}) for a Category 1 Hurricane versus Time at Coordinate (0,0)

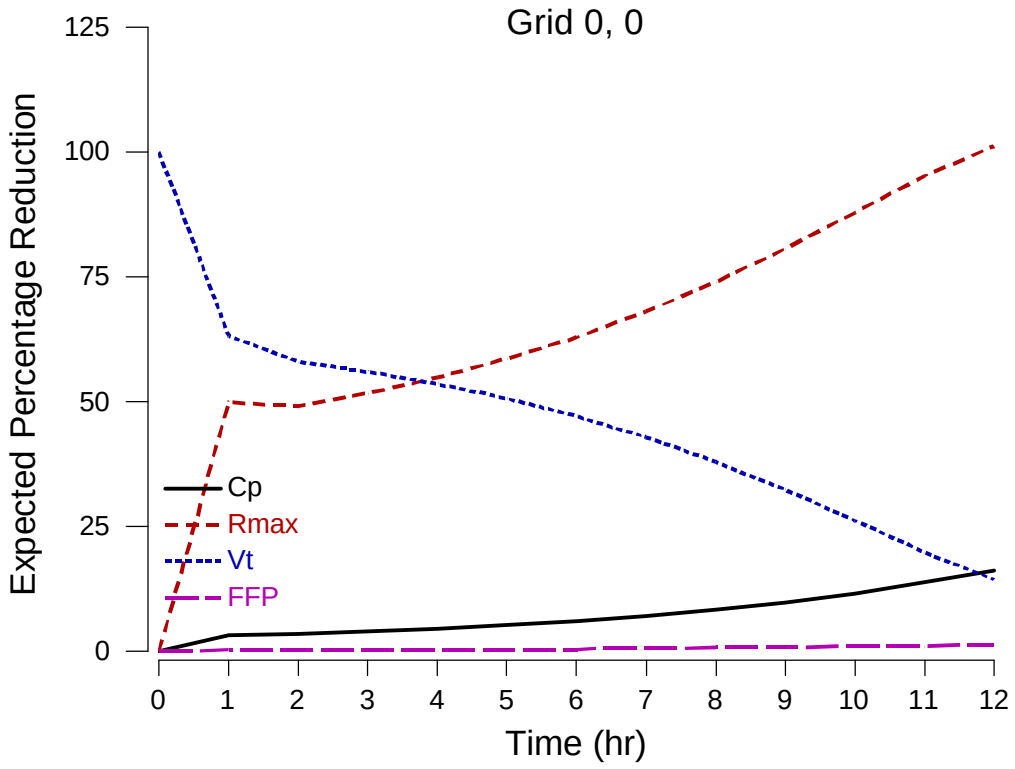

Figure 37. Expected Percentage Reductions in the Var(V_{Total}) for a Category 5 Hurricane versus Time at Coordinate (0,0)

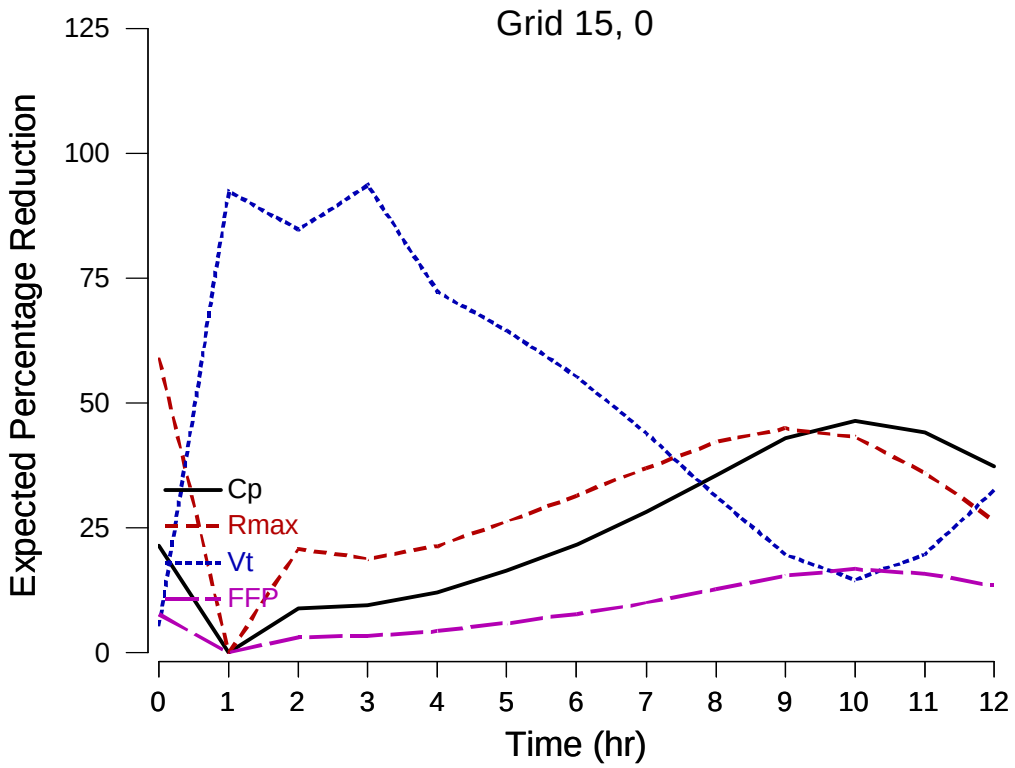

Figure 38. Expected Percentage Reductions in the Var(V_{Total}) for a Category 1 Hurricane versus Time at Coordinate (15,0)

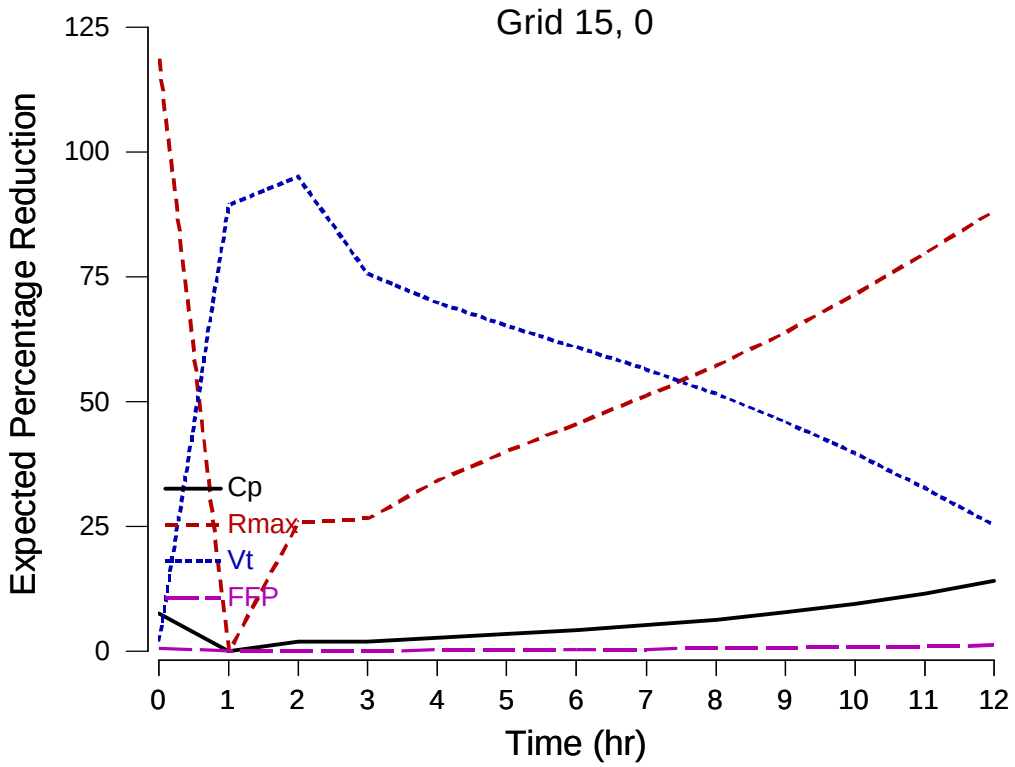

Figure 39. Expected Percentage Reductions in the Var(V_{Total}) for a Category 5 Hurricane versus Time at Coordinate (15,0)

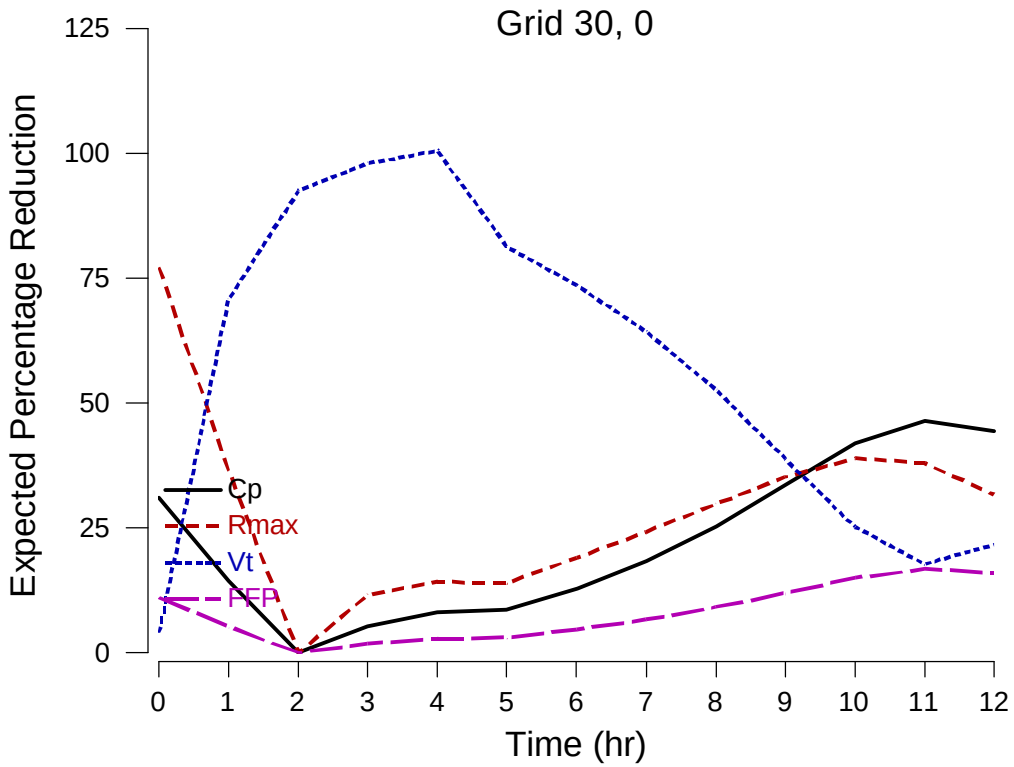

Figure 40. Expected Percentage Reductions in the Var(V_{Total}) for a Category 1 Hurricane versus Time at Coordinate (30,0)

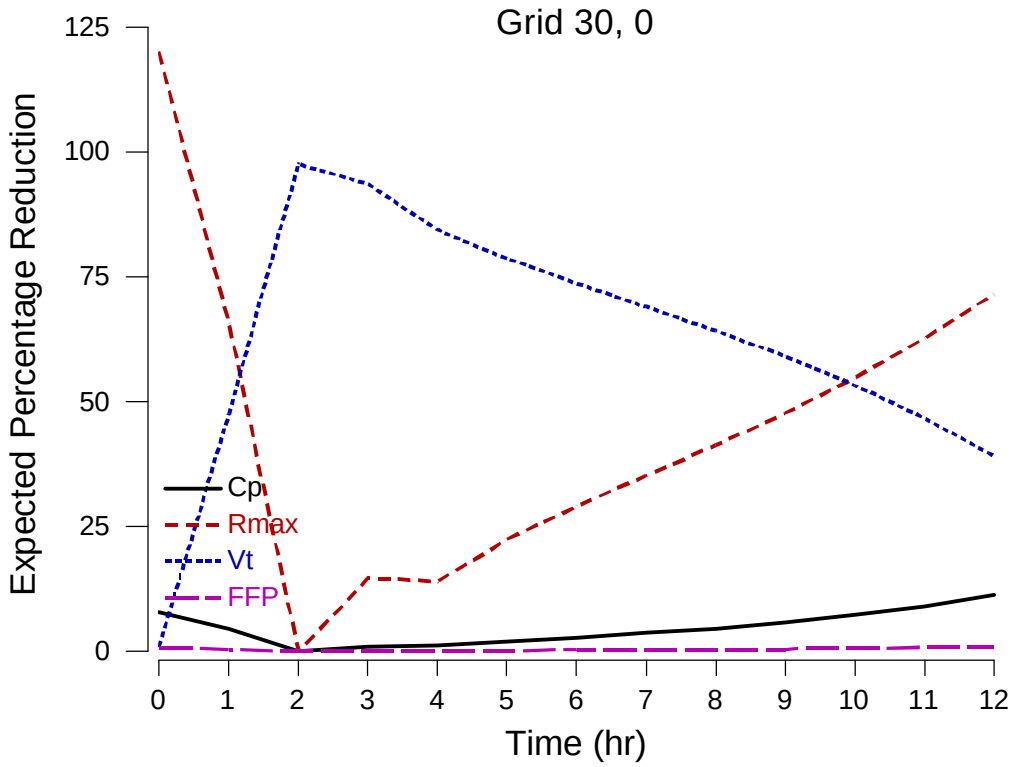

Figure 41. Expected Percentage Reductions in the Var(V_{Total}) for a Category 5 Hurricane versus Time at Coordinate (30,0)

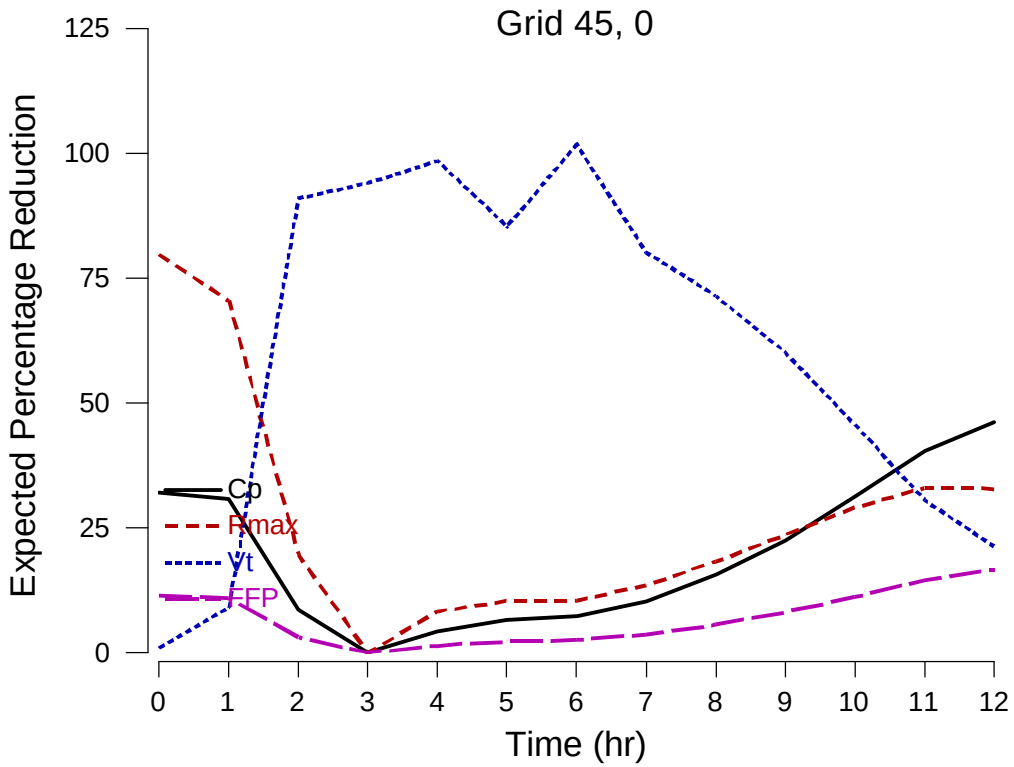

Figure 42. Expected Percentage Reductions in the Var(V_{Total}) for a Category 1 Hurricane versus Time at Coordinate (45,0)

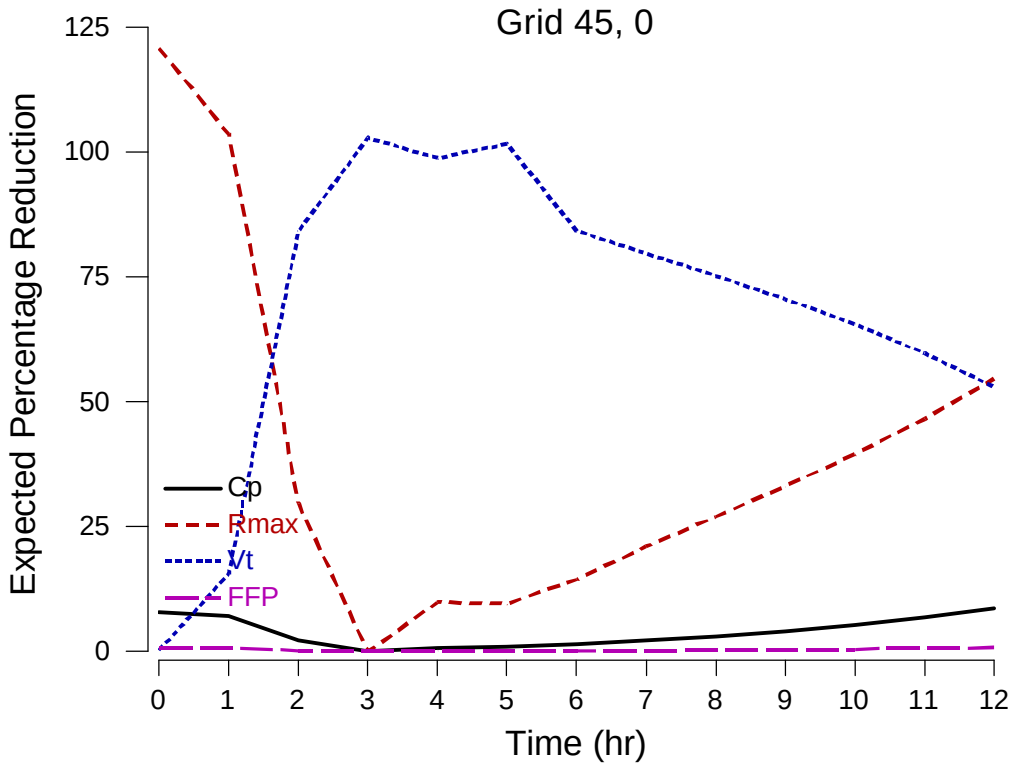

Figure 43. Expected Percentage Reductions in the Var(V_{Total}) for a Category 5 Hurricane versus Time at Coordinate (45,0)

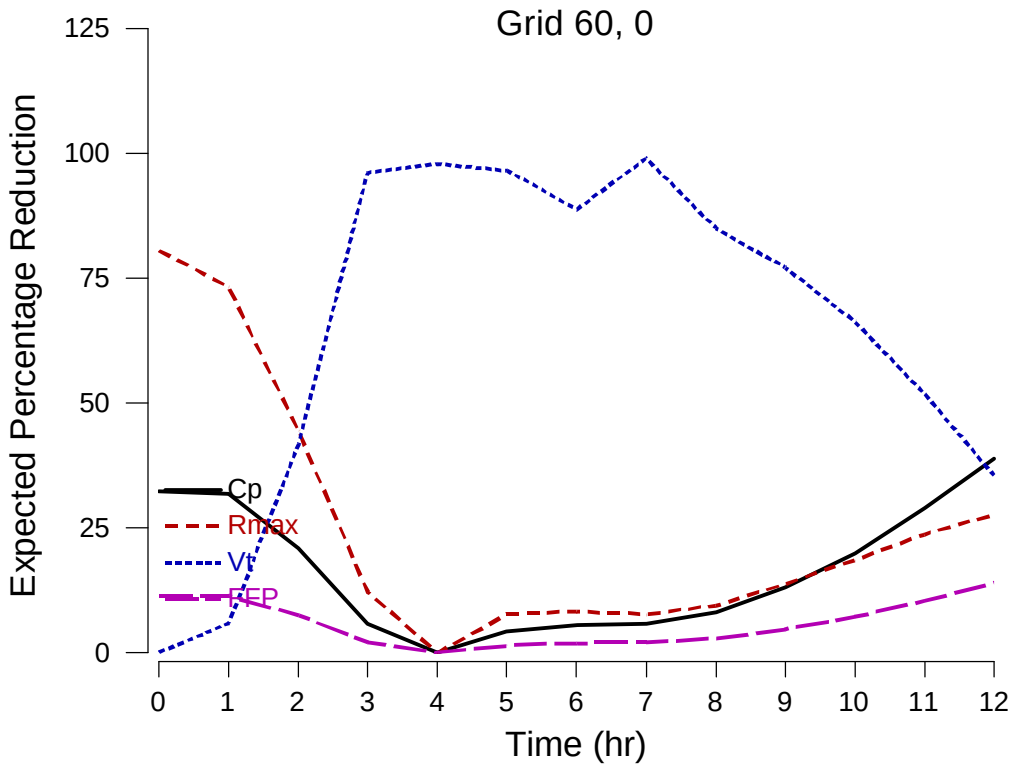

Figure 44. Expected Percentage Reductions in the Var(V_{Total}) for a Category 1 Hurricane versus Time at Coordinate (60,0)

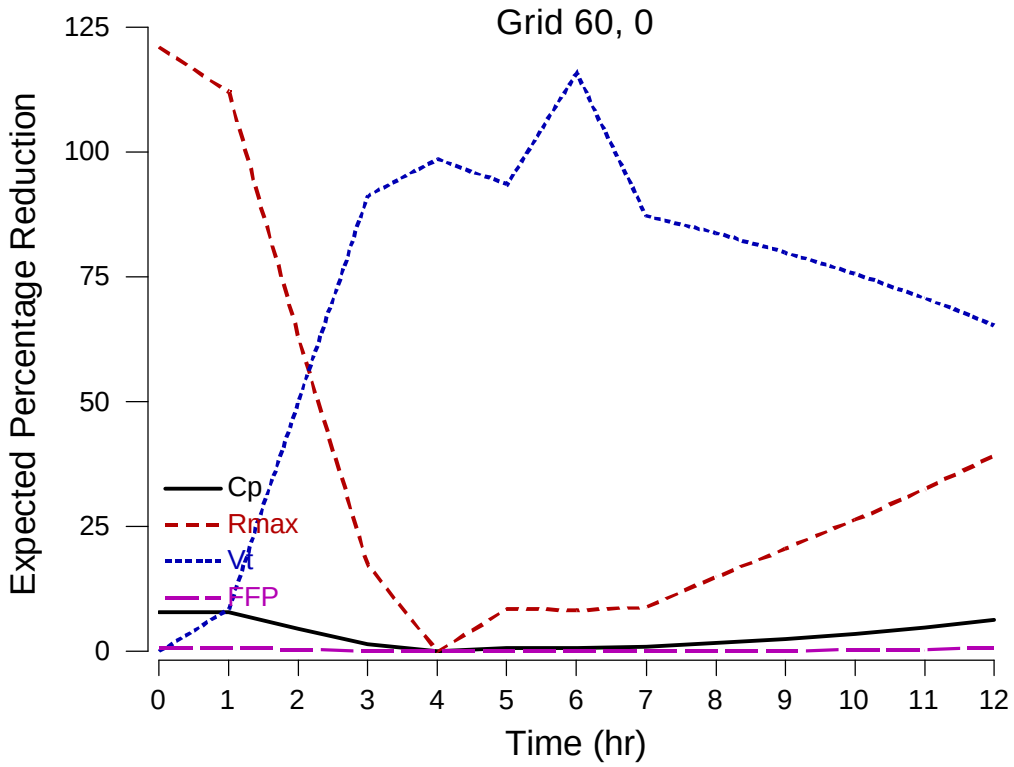

Figure 45. Expected Percentage Reductions in the Var(V_{Total}) for a Category 5 Hurricane versus Time at Coordinate (60,0)

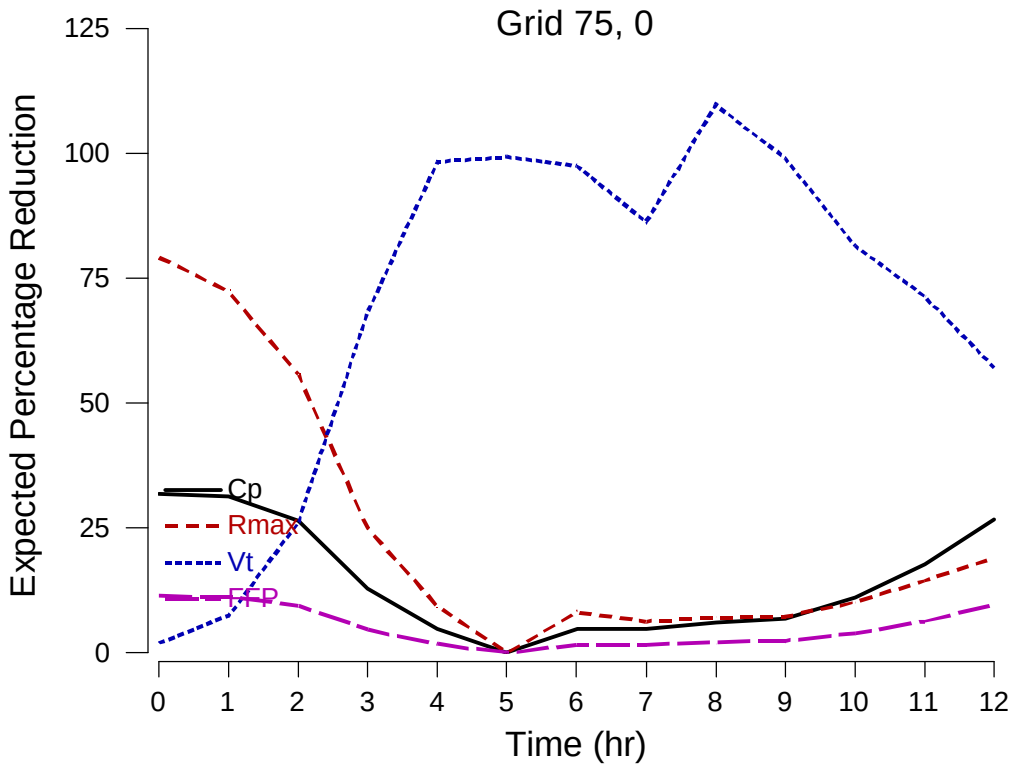

Figure 46. Expected Percentage Reductions in the Var(V_{Total}) for a Category 5 Hurricane versus Time at Coordinate (75,0)

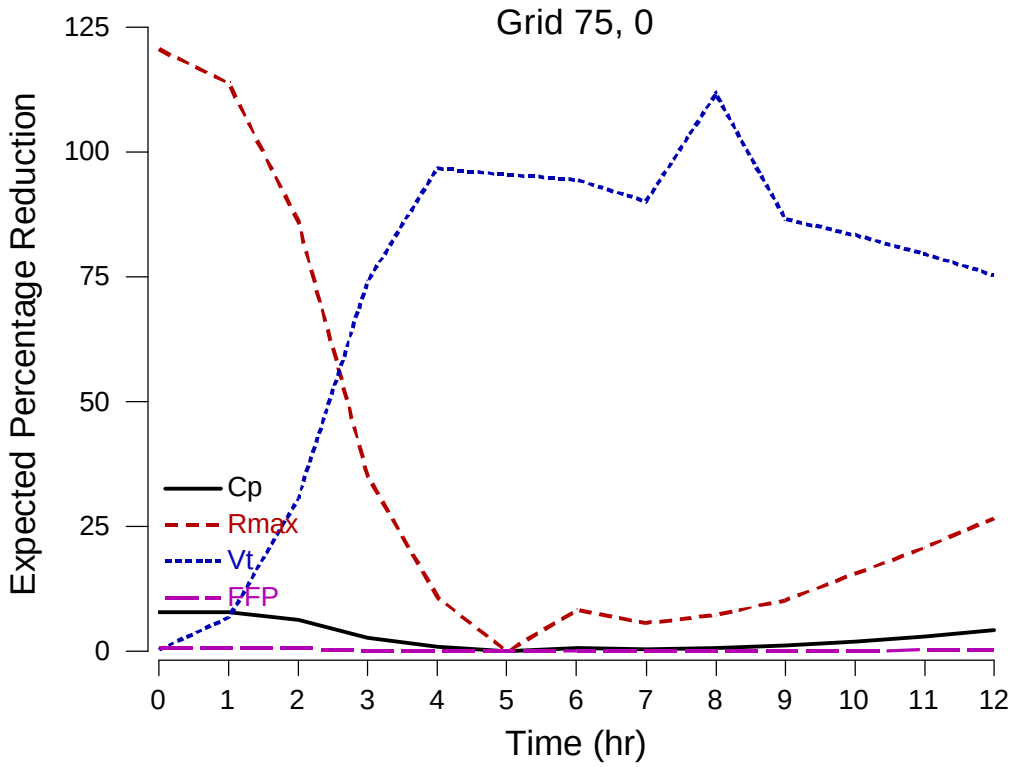

Figure 47. Expected Percentage Reductions in the Var(V_{Total}) for a Category 5 Hurricane versus Time at Coordinate (75,0)

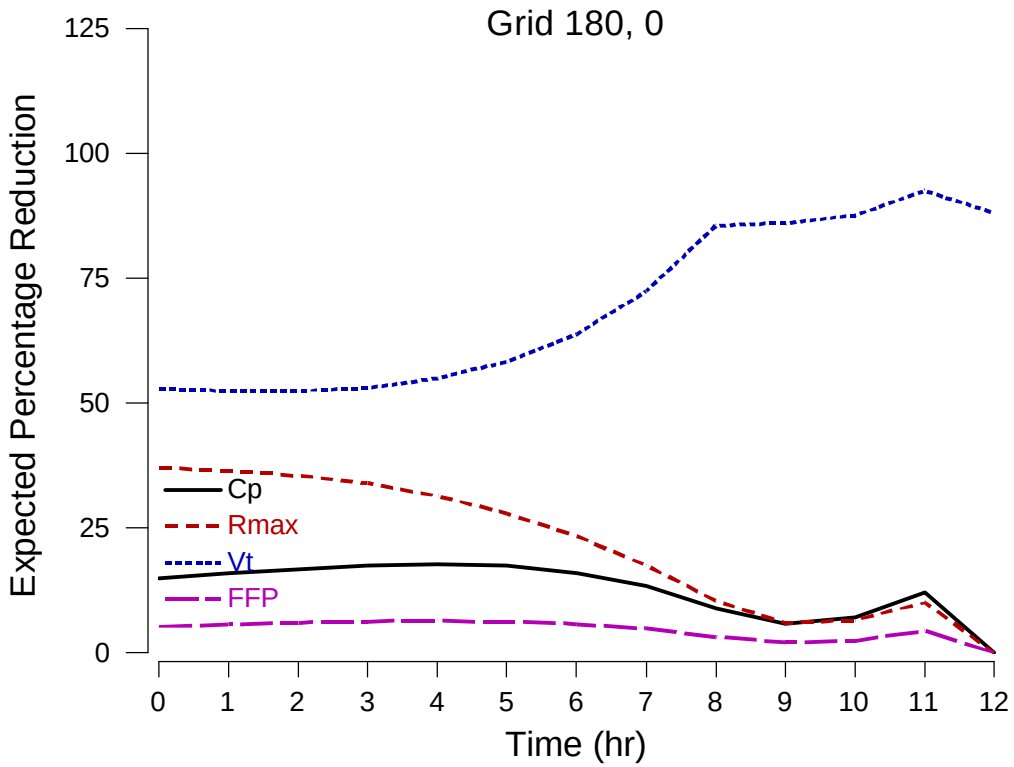

Figure 48. Expected Percentage Reductions in the Var(V_{Total}) for a Category 1 Hurricane versus Time at Coordinate (180,0)

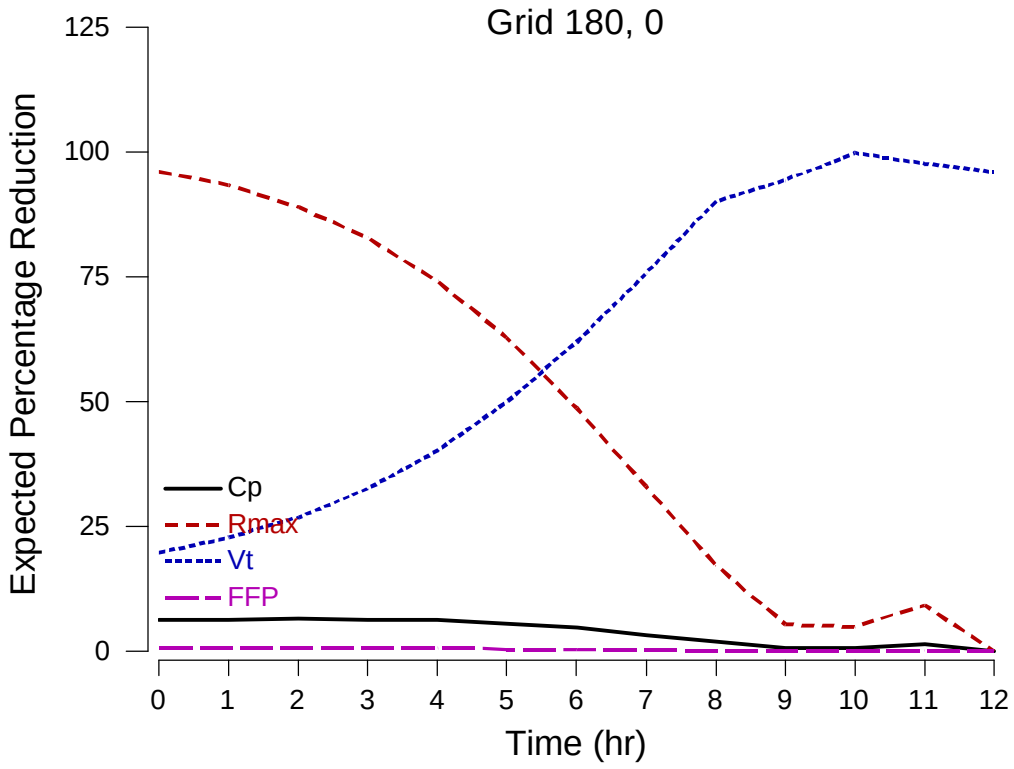

Figure 49. Expected Percentage Reductions in the Var(V_{Total}) for a Category 5 Hurricane versus Time at Coordinate (180,0)

Table 14. Summary of the Contribution of the Four Input Parameters to the Uncertainty in V_{Total} at Coordinate (30, 0) over the 12hr Time Period

	Category 1	Category 5
CP	• Contribution decreases to t=2hr when the eye of the storm is located approximately at (30, 0) • Increases throughout the remaining times, reaching a maximum of 46.5% at t=11hr • Relative contribution of CP is much greater throughout for a Category 1 than for a Category 5	• Contribution decreases to t=2hr when the eye of the storm is located approximately at (30, 0) • Increases throughout the remaining times, reaching a maximum of 8.8% at t=12hr • Relative contribution of CP gradually increases throughout the remaining times but remains less than for a Category 1
Rmax	• Maximum contribution (77.2%) at t=0hr • Decreases to 0% contribution at t=2hr when the eye of the storm is located approximately at (30, 0) • Contribution increases similar to that of CP for t > 3hr to a max of 38.9% • Contribution is much less that for a Category 5	• Maximum contribution (120.0%) at t=0hr • Quickly changes to 65.9% at t-1hr • Decreases to 0% at t=2hr when the eye of the storm is located approximately at (30, 0) • Contribution increases for t > 3hr reaching a maximum of 71.6% at t=12hr • Contribution is greater than for a Category 1.
V_T	• Contribution increases from 4.0% at t=0hr to 100.5% at t=4hr • Decreases to 17.8% at t=11hr and then increases to 21.7% at t=12hr	• Contribution increases from 0.9% at t=0hr to 97.6% at t=2hr • Decreases to 39.1% at t=12hr
FFP	• Pattern is similar to that for CP and Rmax, but lower in magnitude with a contribution of 11.1% at t=0hr and 16.0% at t=12hr	• Contribution FFP is nearly constant throughout the 12hr time period and has very little influence ranging from 0.7% at t=0hr to 1.0% at t=12hr

Table 12 presented a summary of the SA results at coordinate (30, 0). Table 14 contains a similar summary for the UA results at (30, 0). Figures 40 and 41, which give the UA results for (30, 0), are useful in interpreting the summaries in Table 14.

Appendix C contains five complete sets of graphs similar to Figures 36 to 49 for the following coordinates:

- 5mi south of the path of the eye: (0, -5) to (180, -5)
- Path of the eye: (0, 0) to (180, 0)
- 5mi north of the path of the eye: (0, 5) to (180, 5)
- 10mi north of the path of the eye: (0, 10) to (180, 10)
- 15mi north of the path of the eye: (0, 15) to (180, 15)

Rankings of the Input Parameters. The relative importance of the four input parameters as determined by the SA and UA for (30, 0) can be summarized by a simple ranking of each measure from 1 (most important) to 4 (least important). Table 15 presents a side-by-side comparison of the SA and UA rankings of the input parameters by time and storm category.

Equation 3 was used to compute simple correlation coefficients (a.k.a., rank correlation) for the sets of rankings in Table 15 as a measure of agreement between the two sets. These correlations appear in the "Corr" column of that table. Five of the 13 sets of rankings for Category 1 show perfect agreement (correlation = 1.00) while nine of the Category 5 sets have perfect agreement. The negative correlation at t = 2hr for Category 5 occurs when the approximate location of the eye of storm is (30, 0). The corresponding correlations for Category 5 are frequently higher than those for Category 1.

Table 16 is similar in construction to Table 15 with the difference being that the rankings are compared by hurricane category first for SA and then again for UA. The SA correlations are low during the early hours of the hurricanes and then increase to perfect correlation from t = 5hr to 9hr and then decrease to 0. The UA correlations are either 1 or close to 1 until t = 11hr, where they fall off abruptly.

The reader is cautioned not to attempt to generalize the results in Tables 13 and 16 for (30, 0), which is directly on the path of the eye as these rankings are affected by the location of the grid vertex. Two other sets of coordinates to the right of the hurricane, (15, 10) and (30, 10), have been provided for the reader to make similar comparisons. These rankings and correlations are given in Tables 17 to 20.

There are many comparisons that could be made among the rankings in Tables 15 to 20, but only the following brief observations are presented.

- All rankings generally have FFP in either 3rd or 4th place
- There is better agreement between the rankings for the two set of coordinates to the right of the hurricane than there is between these rankings and those directly on the path of the eye
- V_T and Rmax are the most important input variables for Categories 1 and 5 at (30, 0), but CP is much closer to these two parameters for a Category 5 than for a Category 1 Rmax is the most important variable for Category 1 at (15, 10) followed by CP and V_T
- Rmax is the most important variable for Category 5 at (15, 10) followed closely by V_T with CP a distant third
- Rmax is the most important variable for Category 1 at (30, 10) followed closely by CP and V_T
- Rmax and V_T are the most important input variables for Category 5 at (30, 10) with CP a distant third

The discussion of uncertainty analysis concludes with a revisit to loss cost considered in the SA presentation.

Uncertainty Analysis for Loss Cost. The loss cost calculations covered earlier were also subjected to an uncertainty analysis. As with SA, loss costs were summed hourly over all vertices with $X \geq 15$mi to get total loss cost at time t. An UA could have been performed to determine the influence of the four input parameters in Table 1 on hourly loss costs in the same manner that was just illustrated for V_{Total}, but these are of limited utility. Thus, UA will be considered only for maximum total loss cost during the 12hr period.

In particular, the UA was performed on the maximum total loss cost associated with each of the n=100 LHS input vectors. Figures 33 and 34 showed these n=100 responses as estimated cumulative distribution functions for total loss cost for Category 1 and 5, respectively. The contributions of the four input parameters in Table 1 to the uncertainty represented in these figures are the focus of the UA for loss cost.

The expected percentage reduction in uncertainty associated with loss cost is calculated by following the eight steps that were given previously. Table 21 summarizes these percentages by hurricane category and also gives their corresponding ranks from 1 (most influential) to 4 (least influential). Note that CP is by far the most influential for Category 1, but FFP finishes a strong second. On the other hand, Rmax is clearly the most influential for Category 5 with CP and V_T having nearly identical influence. FFP is the least influential for Category 5.

The rankings in Table 21 for Category 1 are the same as those previously given in Table 13 for the SA. The Category 5 results differ only in having the ranks of 3 and 4 reversed in these two tables.

Category 1 results in Tables 13 and 21 are particularly noteworthy since FFP was near the bottom of the rankings in the SA and UA for V_{Total}. The loss cost results indicate that parameters that were not particularly influential for wind speed can be influential for loss cost. One possible explanation for this behavior is that the loss cost function greatly changes the nature of the relationship between the input parameters and the output by setting any wind speed $\leq$ 69.39mph to \$0 and any wind speed $\geq$ 121.43mph to \$99,000. It may be that the wind speeds that are not subjected to these truncations for a Category 1 hurricane are influenced by FFP, thus identifying FFP as influential.

The sensitivity of loss cost to FFP for a Category 1 hurricane is shown in Figure 50. The cumulative distribution function (cdf) for loss cost for a Category 1 hurricane previously given in Figure 33 is repeated in this figure with the label "LHS." Recall that this cdf was produced by allowing FFP to vary according to a triangular distribution between 1010mB and 1016mB with a mean of 1013mB. The cdf labeled "1013mB" in Figure 50 corresponds to holding FFP fixed at 1013mB (this is the fixed value typically used for far field pressure).

The cdfs for LHS and 1013mB are quite close, since the mean of the triangular distribution was 1013mB and 89% of the FFP values in the LHS were between 1011mB and 1015mb, which is a very narrow window for uncertainty in FFP. The cdf in Figure 49 with the label "1016mB" corresponds to holding FFP fixed at 1016mB. The other cdfs in Figure 50 correspond to holding FFP fixed at 1018mB and 1020mB. The summary statistics for these five cdfs are given in Table 22.

Table 15. Correlations of the SA and UA Rankings of the Input Parameters by Time and Hurricane Category at Coordinates (30, 0)

		Category 1					Category 5				
Time		**CP**	**Rmax**	**V_T**	**FFP**	**Corr**	**CP**	**Rmax**	**V_T**	**FFP**	**Corr**
0hr	**SA**	2	1	4	3	1.00	2	1	3	3	0.94
	UA	2	1	4	3		2	1	3	4	
1hr	**SA**	2	3	1	4	0.80	3	1	2	4	1.00
	UA	3	2	1	4		3	1	2	4	
2hr	**SA**	3	1	2	4	0.26	2	1	4	3	-0.77
	UA	2	2	1	2		2	2	1	2	
3hr	**SA**	2	4	1	3	0.40	2	3	1	4	0.80
	UA	3	2	1	4		3	2	1	4	
4hr	**SA**	2	3	1	4	0.80	3	2	1	4	1.00
	UA	3	2	1	4		3	2	1	4	
5hr	**SA**	3	2	1	4	1.00	3	2	1	4	1.00
	UA	3	2	1	4		3	2	1	4	
6hr	**SA**	3	2	1	4	1.00	3	2	1	4	1.00
	UA	3	2	1	4		3	2	1	4	
7hr	**SA**	3	2	1	4	1.00	3	2	1	4	1.00
	UA	3	2	1	4		3	2	1	4	
9hr	**SA**	3	2	1	4	1.00	3	2	1	4	1.00
	UA	3	2	1	4		3	2	1	4	
10hr	**SA**	2	1	3	4	0.40	3	2	1	4	1.00
	UA	3	2	1	4		3	2	1	4	
11hr	**SA**	2	1	4	3	0.60	3	1	2	4	1.00
	UA	1	2	3	4		3	1	2	4	
12hr	**SA**	1	2	4	3	0.80	3	1	2	4	1.00
	UA	1	2	3	4		3	1	2	4	

Table 16. Correlations of the Category 1 and 5 Rankings of the Input Parameters by Time and Analysis Type at Coordinate (30, 0)

		Sensitivity Analysis					Uncertainty Analysis				
Time		**CP**	**Rmax**	**V_T**	**FFP**	**Corr**	**CP**	**Rmax**	**V_T**	**FFP**	**Corr**
0hr	**Cat 1**	2	1	4	3	0.94	2	1	4	3	0.80
	Cat 5	2	1	3	3		2	1	3	4	
1hr	**Cat 1**	2	3	1	4	0.40	3	2	1	4	0.80
	Cat 5	3	1	2	4		3	1	2	4	
2hr	**Cat 1**	3	1	2	4	0.40	2	2	1	2	1.00
	Cat 5	2	1	4	3		2	2	1	2	
3hr	**Cat 1**	2	4	1	3	0.80	3	2	1	4	1.00
	Cat 5	2	3	1	4		3	2	1	4	
4hr	**Cat 1**	2	3	1	4	0.80	3	2	1	4	1.00
	Cat 5	3	2	1	4		3	2	1	4	
5hr	**Cat 1**	3	2	1	4	1.00	3	2	1	4	1.00
	Cat 5	3	2	1	4		3	2	1	4	
6hr	**Cat 1**	3	2	1	4	1.00	3	2	1	4	1.00
	Cat 5	3	2	1	4		3	2	1	4	
7hr	**Cat 1**	3	2	1	4	1.00	3	2	1	4	1.00
	Cat 5	3	2	1	4		3	2	1	4	
9hr	**Cat 1**	3	2	1	4	1.00	3	2	1	4	1.00
	Cat 5	3	2	1	4		3	2	1	4	
10hr	**Cat 1**	2	1	3	4	0.40	3	2	1	4	1.00
	Cat 5	3	2	1	4		3	2	1	4	
11hr	**Cat 1**	2	1	4	3	0.40	1	2	3	4	0.40
	Cat 5	3	1	2	4		3	1	2	4	
12hr	**Cat 1**	1	2	4	3	0.00	1	2	3	4	0.40
	Cat 5	3	1	2	4		3	1	2	4	

Table 17. Correlations of the SA and UA Rankings of the Input Parameters by Time and Hurricane Category at Coordinate (15, 10)

		Category 1					Category 5				
Time		**CP**	**Rmax**	**V_T**	**FFP**	**Corr**	**CP**	**Rmax**	**V_T**	**FFP**	**Corr**
0hr	**SA**	1	2	4	3	0.80	2	1	4	3	1.00
	UA	2	1	4	3		2	1	4	3	
1hr	**SA**	2	1	4	3	1.00	2	1	4	3	0.80
	UA	2	1	4	3		2	1	3	4	
2hr	**SA**	1	4	2	3	0.00	3	2	1	4	1.00
	UA	3	2	1	4		3	2	1	4	
3hr	**SA**	3	2	1	4	1.00	3	2	1	4	1.00
	UA	3	2	1	4		3	2	1	4	
4hr	**SA**	3	2	1	4	1.00	3	2	1	4	1.00
	UA	3	2	1	4		3	2	1	4	
5hr	**SA**	3	2	1	4	1.00	3	2	1	4	1.00
	UA	3	2	1	4		3	2	1	4	
6hr	**SA**	3	2	1	4	1.00	3	2	1	4	1.00
	UA	3	2	1	4		3	2	1	4	
7hr	**SA**	3	1	2	4	0.80	3	1	2	4	0.80
	UA	3	2	1	4		3	2	1	4	
9hr	**SA**	2	1	3	4	1.00	3	1	2	4	1.00
	UA	2	1	3	4		3	1	2	4	
10hr	**SA**	2	1	4	3	0.80	3	1	2	4	1.00
	UA	2	1	3	4		3	1	2	4	
11hr	**SA**	2	1	4	3	0.80	3	1	2	4	1.00
	UA	1	2	4	3		3	1	2	4	
12hr	**SA**	1	2	4	3	1.00	3	1	2	4	1.00
	UA	1	2	4	3		3	1	2	4	

Table 18. Correlations of the Category 1 and 5 Rankings of the Input Parameters by Time and Analysis Type at Coordinate (15, 10)

		Sensitivity Analysis					Uncertainty Analysis				
Time		**CP**	**Rmax**	**V_T**	**FFP**	**Corr**	**CP**	**Rmax**	**V_T**	**FFP**	**Corr**
0hr	**Cat 1**	1	2	4	3	0.80	2	1	4	3	1.00
	Cat 5	2	1	4	3		2	1	4	3	
1hr	**Cat 1**	2	1	4	3	1.00	2	1	4	3	0.80
	Cat 5	2	1	4	3		2	1	3	4	
2hr	**Cat 1**	1	4	2	3	0.00	3	2	1	4	1.00
	Cat 5	3	2	1	4		3	2	1	4	
3hr	**Cat 1**	3	2	1	4	1.00	3	2	1	4	1.00
	Cat 5	3	2	1	4		3	2	1	4	
4hr	**Cat 1**	3	2	1	4	1.00	3	2	1	4	1.00
	Cat 5	3	2	1	4		3	2	1	4	
5hr	**Cat 1**	3	2	1	4	1.00	3	2	1	4	1.00
	Cat 5	3	2	1	4		3	2	1	4	
6hr	**Cat 1**	3	2	1	4	1.00	3	2	1	4	1.00
	Cat 5	3	2	1	4		3	2	1	4	
7hr	**Cat 1**	3	1	2	4	1.00	3	2	1	4	1.00
	Cat 5	3	1	2	4		3	2	1	4	
9hr	**Cat 1**	2	1	3	4	0.80	2	1	3	4	0.80
	Cat 5	3	1	2	4		3	1	2	4	
10hr	**Cat 1**	2	1	4	3	0.40	2	1	3	4	0.80
	Cat 5	3	1	2	4		3	1	2	4	
11hr	**Cat 1**	2	1	4	3	0.40	1	2	4	3	0.00
	Cat 5	3	1	2	4		3	1	2	4	
12hr	**Cat 1**	1	2	4	3	0.00	1	2	4	3	0.00
	Cat 5	3	1	2	4		3	1	2	4	

Table 19. Correlations of the SA and UA Rankings of the Input Parameters by Time and Hurricane Category at Coordinate (30, 10)

		Category 1					Category 5				
Time		**CP**	**Rmax**	**V_T**	**FFP**	**Corr**	**CP**	**Rmax**	**V_T**	**FFP**	**Corr**
0hr	**SA**	2	1	4	3	1.00	2	1	4	3	1.00
	UA	2	1	4	3		2	1	4	3	
1hr	**SA**	2	3	1	4	0.40	3	1	2	4	1.00
	UA	3	1	2	4		3	1	2	4	
2hr	**SA**	2	1	4	3	0.40	2	1	4	3	0.40
	UA	3	1	2	4		3	1	2	4	
3hr	**SA**	1	4	2	3	0.00	3	2	1	4	1.00
	UA	3	2	1	4		3	2	1	4	
4hr	**SA**	3	2	1	4	1.00	3	2	1	4	1.00
	UA	3	2	1	4		3	2	1	4	
5hr	**SA**	3	2	1	4	1.00	3	2	1	4	1.00
	UA	3	2	1	4		3	2	1	4	
6hr	**SA**	3	2	1	4	1.00	3	2	1	4	1.00
	UA	3	2	1	4		3	2	1	4	
7hr	**SA**	3	2	1	4	1.00	3	2	1	4	1.00
	UA	3	2	1	4		3	2	1	4	
9hr	**SA**	3	2	1	4	1.00	3	2	1	4	1.00
	UA	3	2	1	4		3	2	1	4	
10hr	**SA**	3	1	2	4	0.80	3	2	1	4	1.00
	UA	3	2	1	4		3	2	1	4	
11hr	**SA**	2	1	4	3	0.60	3	1	2	4	0.80
	UA	1	2	3	4		3	2	1	4	
12hr	**SA**	1	2	4	3	0.80	3	1	2	4	1.00
	UA	1	2	3	4		3	1	2	4	

Table 20. Correlations of the Category 1 and 5 Rankings of the Input Parameters by Time and Analysis Type at Coordinate (30, 10)

		Sensitivity Analysis					Uncertainty Analysis				
Time		**CP**	**Rmax**	**V_T**	**FFP**	**Corr**	**CP**	**Rmax**	**V_T**	**FFP**	**Corr**
0hr	**Cat 1**	2	1	4	3	1.00	2	1	4	3	1.00
	Cat 5	2	1	4	3		2	1	4	3	
1hr	**Cat 1**	2	3	1	4	0.40	3	1	2	4	1.00
	Cat 5	3	1	2	4		3	1	2	4	
2hr	**Cat 1**	2	1	4	3	1.00	3	1	2	4	1.00
	Cat 5	2	1	4	3		3	1	2	4	
3hr	**Cat 1**	1	4	2	3	0.00	3	2	1	4	1.00
	Cat 5	3	2	1	4		3	2	1	4	
4hr	**Cat 1**	3	2	1	4	1.00	3	2	1	4	1.00
	Cat 5	3	2	1	4		3	2	1	4	
5hr	**Cat 1**	3	2	1	4	1.00	3	2	1	4	1.00
	Cat 5	3	2	1	4		3	2	1	4	
6hr	**Cat 1**	3	2	1	4	1.00	3	2	1	4	1.00
	Cat 5	3	2	1	4		3	2	1	4	
7hr	**Cat 1**	3	2	1	4	1.00	3	2	1	4	1.00
	Cat 5	3	2	1	4		3	2	1	4	
9hr	**Cat 1**	3	2	1	4	1.00	3	2	1	4	1.00
	Cat 5	3	2	1	4		3	2	1	4	
10hr	**Cat 1**	3	1	2	4	0.80	3	2	1	4	1.00
	Cat 5	3	2	1	4		3	2	1	4	
11hr	**Cat 1**	2	1	4	3	0.40	1	2	3	4	0.20
	Cat 5	3	1	2	4		3	2	1	4	
12hr	**Cat 1**	1	2	4	3	0.00	1	2	3	4	0.40
	Cat 5	3	1	2	4		3	1	2	4	

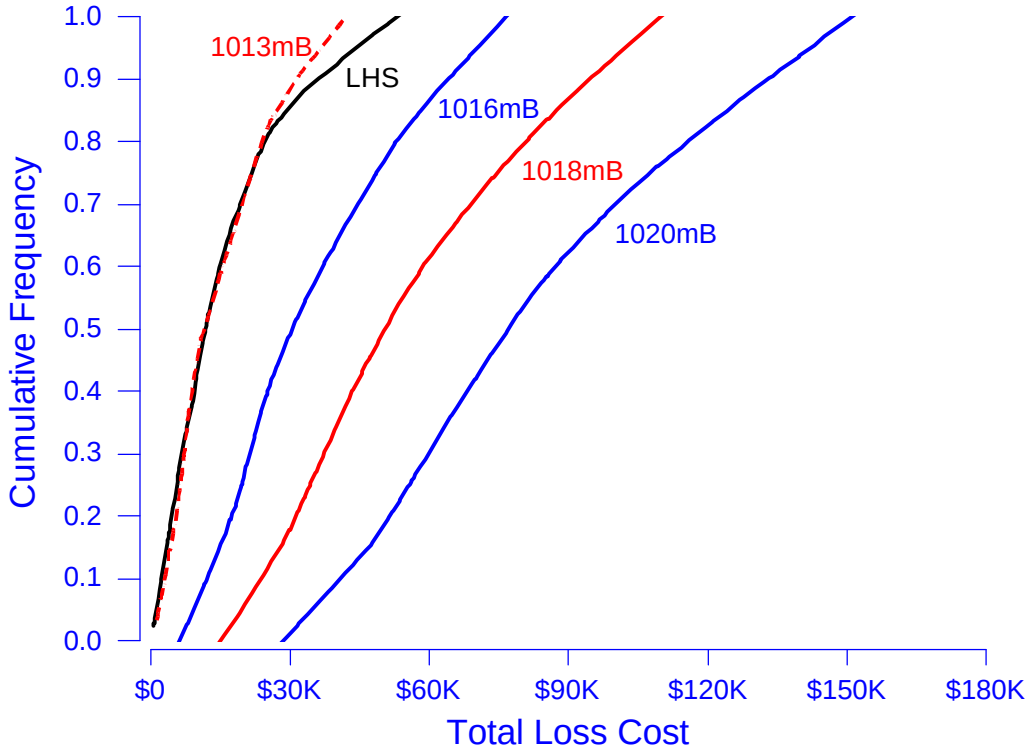

Figure 50. Distribution of Total Loss Cost for a Category 1 Hurricane

Table 21. Percentage Contribution to the Uncertainty in Total Loss Cost by Category of Hurricane

	Category 1				Category 5			
	CP	**Rmax**	**V_T**	**FFP**	**CP**	**Rmax**	**V_T**	**FFP**
Percentage	92.5%	10.1%	1.8%	28.8%	8.2%	48.5%	7.0%	0.8%
Rank	1	3	4	2	2	1	3	4

Table 22. Loss Cost Statistics for Various Values of FFP

FFP	Mean	St. Dev.	Minimum	Maximum
LHS	$15,384	$12,957	$ 546	$ 56,274
1013mB	$14,739	$10,786	$ 1,294	$ 44,631
1016mB	$34,981	$19,494	$ 5,752	$ 90,963
1018mB	$55,715	$26,427	$13,138	$131,364
1020mB	$83,021	$34,089	$25,179	$179,741

Note that the most conservative estimates in Table 22 correspond to holding FFP fixed at 1013mB. Raising this value to just 1016mB increases the mean loss cost by a factor of 2.37 and the maximum by a factor of 2.04. The respective factors for 1020mB are 5.63 and 4.03. These results are quite illuminating in that loss cost in this simple model is quite sensitive to the value of FFP for the most frequently occurring hurricanes. Note: this is not a parameter that has been subjected to variation in the year 2000 submissions.

There are measures other than the one based on Equation 20 that can be used in uncertainty analysis. Iman and Hora (1990) present robust measures that can be used when the response variable has outlying observations that

make it difficult to get a reliable estimate of the variance. Several researchers have offered measures for use in fault tree analysis: Bhattacharyya and Amed (1982), Bier (1983), Wheeler and Spulak (1985), and Nakashima and Yamato (1982).

Other applications of uncertainty analysis can be found in Iman and Conover (1980), Iman and Helton (1988), and Iman, Helton, and Campbell (1990a, 1990b). Appendix D contains a listing of 110 references to other applications of sensitivity and uncertainty analysis.

Summary. This report has provided a detailed sensitivity analysis/uncertainty analysis description for a simple Rankine-vortex wind field, cubic damage function and nominal insurance aspects. The intent is obviously not to provide another model for loss estimation purposes but to illustrate the implementation of appropriate statistical methodologies for doing SA/UA. Latin hypercube sampling designs with PCC/SRC analyses and a calculation for the expected percentage reduction in uncertainty provide viable methodologies to address two key questions:

- What is the change in the response(s) of a model to changes in model inputs and specifications?
- What is the variation in model output resulting from the collective variation in the model inputs?

This demonstration analysis has illustrated that the relative importance of input variables is not necessarily the same for sensitivity and uncertainty analyses and that the relative rankings are dependent on the intensity of storm. This demonstration serves as the basis for a Form B-type module addition to facilitate model-to-model comparisons while quantifying some key aspects of models. Subject to Commission approval, it is anticipated that a set of runs would be made by each modeler as part of the modeler approval process.

Cited References

1. Anthes, R. A. (1982). **Tropical Cyclones, Their Evolution, Structure, and Effects**. Boston, American Meteorological Society, 208pp.

2. Bhattacharya, A. K. and Amed, S. (1982). “Establishing Data Requirements for Plant Probabilistic Risk Assessment,” *Transactions of the American Nuclear Society*, 43, 477-478.

3. Bier, V. M. (1983). “A Measure of Uncertainty Importance for Components in Fault Trees,” *Transactions of the 1983 Winter Meeting of the American Nuclear Society*, 384-385.

4. Fletcher, C. H., Redmond, B. M., Barnes, G.M. and Schroeder, T. A. (1995), “Marine Flooding on the Coast of Kaua'i during Hurricane Iniki: Hindcasting Inundation Components and Delineating Overwash” *J. Coastal Res*., 11, 1, 188-204.

5. Holliday, C. (1969). "On the Maximum Sustained Winds Occurring in Atlantic Hurricanes," ESSA Tech. Memo. WBTM-SR-45, U.S. Weather Bureau, Southern Region, May 1969, 6 pp.

6. Iman, R. L. (1999). "Latin Hypercube Sampling," **Encyclopedia of Statistical Sciences, Update Volume 3**, Wiley, NY, 408-411.

7. Iman, R. L. (1987). "A Matrix-Based Approach to Uncertainty and Sensitivity Analysis for Fault Trees," *Risk Analysis*, 7(1), 21-33.

8. Iman, R. L. and Conover (1982). "A Distribution-Free Approach to Inducing Rank Correlation Among Input Variables, "*Communications in Statistics*, B11(3), 311-334.

9. Iman, R. L. and Conover, W. J. (1980). "Small Sample Sensitivity Analysis Techniques for Computer Models, with an Application to Risk Assessment," *Communications in Statistics*, A9(17), p. 1749-1842. "Rejoinder to Comments," 1863-1874.

10. Iman, R. L. and Davenport, J. M. (1982). "Rank Correlation Plots for Use with Correlated Input Variables," *Communications in Statistics*, B11(3), 335-360.

11. Iman, R. L. and Helton, J. C. (1988). "An Investigation of Uncertainty and Sensitivity Analysis Techniques for Computer Models," *Risk Analysis*, 8(1), 71-90.

12. Iman, R. L., Helton, J. C., and Campbell, J. E. (1990). "An Approach to Sensitivity Analysis of Computer Models, Part l. Introduction, Input Variable Selection and Preliminary Variable Assessment," *Journal of Quality Technology*, 13(3), 174-183.

13. Iman, R. L., Helton, J. C., and Campbell, J. E. (1990). "An Approach to Sensitivity Analysis of Computer Models, Part 2. Ranking of Input Variables, Response Surface Validation, Distribution Effect and Technique Synopsis," *Journal of Quality Technology*, 13(4), 232-40.

14. Iman, R. L. and Hora, S. C. (1990). "A Robust Measure of Uncertainty Importance for Use in Fault Tree System Analysis," *Risk Analysis*, 10(3), 401-406.

15. Nakashima, K. and Yamato, K. (1982). “Variance Importance of Systems Components,” *IEEE Transactions on Reliability*, R-31, 99-100.

16. Parzen, E. (1962). **Stochastic Processes**, Holden-Day, San Francisco.

17. Wheeler, T. A. and Spulak, R. G. (1985). “The Importance of Data and Related Uncertainties in Probabilistic Risk Assessments,” *Proceedings of the ANS/ENS International Topical Meeting of Probabilistic Safety Methods and Applications*.